Materials and Design 193 (2020) 108794

Contents lists available at ScienceDirect

Materials and Design

journal homepage: www.elsevier.com/locate/matdes

Bioprinting of 3D *in vitro* skeletal muscle models: A review

Pei Zhuang [a], Jia An [a], Chee Kai Chua [b], Lay Poh Tan [c,*]

[a] Singapore Centre for 3D Printing, School of Mechanical and Aerospace Engineering, Nanyang Technological University, 50 Nanyang Avenue, 639798, Singapore
[b] Engineering Product Development Pillar, Singapore University of Technology and Design, 8 Somapah Rd, 487372 Singapore, Singapore
[c] School of Materials Science and Engineering, Nanyang Technological University, 50 Nanyang Avenue, 639798, Singapore

HIGHLIGHTS

- Recent progress in engineering skeletal muscle models are thoroughly reviewed.
- Design considerations for engineering skeletal muscles are presented.
- Effects of different stimulus on cellular behavior are discussed.
- Bioengineering strategies, especially bioprinting, for 3D skeletal muscle modeling are investigated.
- The major challenges and opportunities are highlighted.

GRAPHICAL ABSTRACT

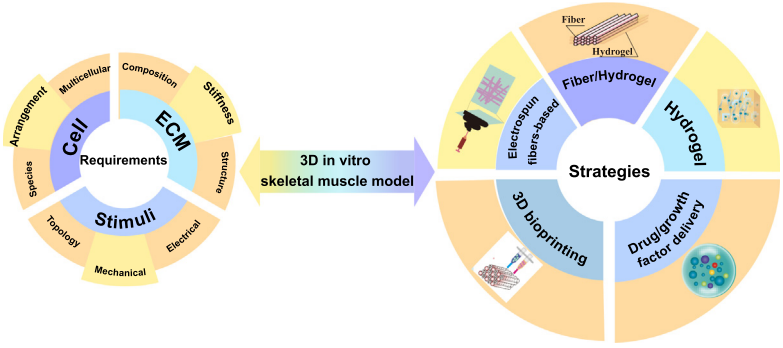

ARTICLE INFO

Article history:
Received 18 October 2019
Received in revised form 6 May 2020
Accepted 7 May 2020
Available online 19 May 2020

Keywords:
3D bioprinting
Skeletal muscle
In vitro model
Bioengineering strategies

ABSTRACT

Recent years have witnessed significant progress in skeletal muscle tissue regeneration. Numerous bioengineering approaches have been implemented to construct *in vitro* skeletal muscle tissues with high fidelity. Nevertheless, an *in vitro* model that is capable of restoring mature muscle, vasculature, and ECM composition to the damaged tissue has yet to be achieved. Herein, we critically review the development and progress in tissue engineering skeletal muscle models. We outline the physiology of native skeletal muscle and the design criteria of engineering biomimetic skeletal muscle tissues are discussed. The influential parameters that modulating skeletal muscle cell behavior are highlighted. Subsequently, we critically review the 3D skeletal muscle models using various bioengineering strategies, including 3D geometrical confinement, electrospinning, porous hydrogels, the controlled cell/molecule delivery, and particularly, 3D bioprinting technology. We draw on specific examples to discuss the merits and limitations of each method. A short description of the challenges and future directions is provided.

Contents

1. Introduction . . . 2
2. Design considerations for engineering skeletal muscle . . . 2
2.1. 3D skeletal muscle context . . . 2

* Corresponding author.
E-mail address: lptan@ntu.edu.sg (L.P. Tan).

https://doi.org/10.1016/j.matdes.2020.108794

2.1.1. Anatomical structure . . . 2
2.1.2. Matrix composition . . . 3
2.1.3. Matrix stiffness . . . 4
2.1.4. Multi-cellular environment . . . 4
2.2. Effect of geometrical confinement on tissue engineering skeletal muscle . . . 5
2.3. Effect of mechanical stimuli on tissue engineering skeletal muscle . . . 5
2.4. Effect of electrical stimuli on tissue engineering skeletal muscle . . . 6
3. Engineering *in vitro* skeletal muscle tissues . . . 8
3.1. Electrospun fibers . . . 8
3.2. Porous hydrogel . . . 9
3.2.1. 3D geometrical confinement . . . 9
3.2.2. Hydrogels with unidirectional channels . . . 11
3.2.3. Hydrogels with external stimuli . . . 11
3.3. Combinatorial effects of fibers and hydrogels . . . 12
3.4. Cell/growth factor delivery in skeletal muscle tissue engineering . . . 12
3.5. 3D bioprinted skeletal muscle tissue . . . 13
4. Challenges and perspectives . . . 17
4.1. Immune response . . . 17
4.2. Multicellular environment and cell source selection . . . 17
4.3. Smart biomaterials . . . 18
4.4. Proper vascularization and innervation . . . 18
4.5. Signaling molecules/drug delivery . . . 18
5. Summary . . . 18
Declaration of competing interest . . . 18
Acknowledgements . . . 18
References . . . 18

1. Introduction

Skeletal muscle, which accounts for 40–45% of an adult human body mass, is innervated by the somatic nervous system and controls voluntary movement and locomotion [1]. Skeletal muscle can be functionally compromised by genetic myopathies, aging, traumatic injuries and tumor ablation. Despite their intrinsic remarkable self-regeneration capability for minor injuries, under some compromised conditions, such as severe traumatic injuries and volumetric muscle loss (VML) with muscle loss over 20%, the regeneration process is significantly suppressed by fibrous scar tissue formation and therefore, causing muscle dysfunction [2,3].

Autologous muscle transfer is considered to be the gold standard for skeletal muscle repair. The grafted healthy tissues adjacent to the injury sites with the dense vascular network and nerve-muscle junction will facilitate muscle regeneration [4]. An alternative to autologous muscle transfer is free functional muscle transfer when no muscle is in the vicinity of the injured tissue can be used. However, the sacrifice of healthy tissues is inevitable with these strategies. Frequently occurred donor site morbidity, insufficient innervation, and complications lead to the failure of full muscle function recovery.

Other alternatives such as the transplantation of muscle precursor cells have been broadly explored [5–8]. The transplantation of satellite cells to the muscle of dystrophin-deficient mdx mice has been observed with remarkable muscle fiber regeneration and contractile functional recovery [6]. However, the low expansion capacity of satellite cells, low cell survival rate potentially caused by poor localization or immune rejection, and limited integration with host tissues await to be addressed.

With preserved native structures that could guide fiber alignment and the vascular networks that could possibly facilitate nutrients transportation and waste removal [9–11], decellularized extracellular matrix (dECM) is recognized as an attractive scaffold platform. However, several as-yet unsolved questions, such as the effect of the cell removal process on biochemical and mechanical properties of dECM, the inconsistent outcomes resulted from the batch-to-batch variation, and the cell migration in large scaffolds, should be considered before further applications.

The poor understanding of the exogenous regeneration process resulted in disappointing muscle regeneration outcomes. A robust and authentic *in vitro* skeletal muscle model to elucidate the pathological mechanism and facilitate the regeneration process is, therefore, in great demand.

By incorporating the exogenous factors (physical, chemical, and electrical cues), tissue engineering scaffolds have achieved remarkable progress in skeletal muscle regeneration. A number of bioengineering strategies have been implemented to construct *in vitro* skeletal muscle tissue models. Here we provide insightful analyses of these *in vitro* skeletal muscle tissue models. Briefly, we begin by presenting the fundamental knowledge of native skeletal muscles. The design requirements for emulating the skeletal muscle environment are discussed. Followed by a comprehensive review of the studies on engineering skeletal muscle tissue models using different strategies, including electrospinning, porous hydrogel, and their combination, cell/growth factor delivery, and especially, the rapidly evolving 3D bioprinting technology. Bioprinting has developed into a more versatile platform and has been adapted to collaborate with many other advanced technologies, for instance, electrospun fibers, microfluidics, spheroids, control release, and multi-nozzle printing. This is greatly pushing the limit of bioprinting technology. Finally, we provide the challenges and future perspectives on engineering *in vitro* skeletal muscle tissue models.

2. Design considerations for engineering skeletal muscle

To engineer the skeletal muscle models that bearing higher fidelity, a myriad of studies has been carried out to decipher the native tissue environment and to identify the key regulators in myogenesis. Herein, we present an overview of 3D skeletal muscle context in terms of anatomical structure, matrix composition, stiffness, and cell-cell interactions. Followed by the discussion over the role of topological, mechanical, and electrical cues in modulating the development and maturation of engineered skeletal muscle tissues.

2.1. 3D skeletal muscle context

2.1.1. Anatomical structure

As depicted in Fig. 1, skeletal muscle consists of highly organized, densely packed myofibers (each represents the multinucleated single muscle cell), abundant blood vessels, nerve, and connective tissue.

Many of the muscle fibers are stacked together, along with the neurons and blood vessels to form a cylindrical bundle, which is known as fascicle. Fascicles are bundled together to form a real muscle. Individual myofiber is covered by a basement membrane, which is continuous with the endomysium connective tissue layer. Myofibrils, derived from the fusion of myoblasts, agglomerate to form myofibers within 20 to 100 μm [12]. Myofibrils consist of repeating sections of sarcomeres. The smallest functional unit of skeletal muscle is sarcomere, which consists of a thick filament made of a protein known as myosin and thin filament made of a protein known as actin. Cell organization in skeletal muscle dictates the tissue function, hence, controlling the matrix structure to induce cell alignment represents the first and foremost step in the myogenic process.

2.1.2. Matrix composition

Extracellular matrix (ECM) functions not only as mechanical support, but also imparts instructive signaling to steer cell behavior [13]. A clear understanding of matrix components could benefit material-based therapies. Generally, skeletal muscle composed of two parts of matrices, the basal lamina, and intramuscular connective tissues. The basal lamina is a sheet-like structure and mostly comprises laminin, collagen IV, nidogen, and perlecan [14]. Connective tissue, with a highly

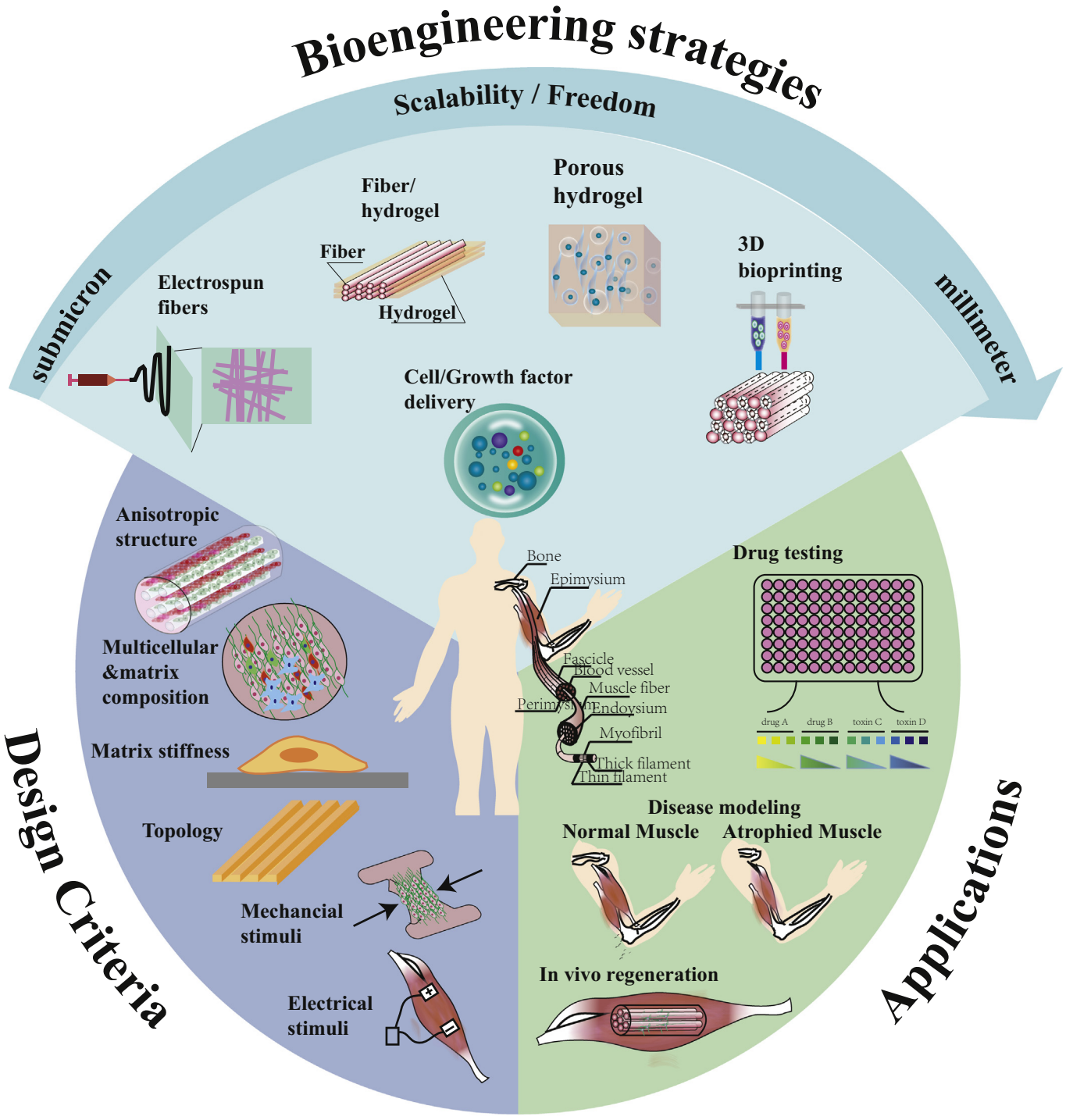

Fig. 1. The overview of the progress of 3D *in vitro* skeletal muscle models, in terms of design criteria, bioengineering strategies, and their potential applications.

organized structure, can be divided into three layers: epimysium, perimysium, and endomysium. Endomysium encloses myofibers and is mainly made of aligned collagen fibers [15]. Muscle fibers bundled together and ensheathed by type I collagen enriched perimysium [16]. These fascicles, interspersed with blood vessels and axons, are wrapped by epimysium, which comprises two wavy sheets of collagen fibrils. Collagen is the major component in skeletal muscles that maintains the structural integrity [17], particularly type I and type III fibrillar collagen. Meanwhile, a minor fraction of type II, V, VI, IX, XII, and XIV have been detected in some specific muscle and species [18].

2.1.3. Matrix stiffness

It is well acknowledged that the mechanical property of substrates exerts significant effects on cell behavior. The differentiation of MSCs is highly controlled by substrate stiffness. They could adopt neuronal phenotype on softer substrate (0.1–1 kPa) [19], and tend to be myogenic on matrices with 10-fold stiffness (8–17 kPa) [20,21]. On a rigid substrate (25–40 kPa), they are likely to be osteogenic [22]. Similarly, skeletal muscle cells are regulated by substrate elasticity as well. The elastic modulus of healthy muscle is 12 kPa, while aging, degenerated and injured muscles possess a higher elastic modulus over 18 kPa [23]. PM Gilbert et al. have identified the importance of satellite niche rigidity by growing freshly isolated muscle stem cells on laminin-coated PEG hydrogel (12 kPa) and rigid plastic dishes (10^6 kPa). Notably, muscle stem cells on softer substrates exhibit superior self-renewal capability *in vitro* and regeneration capacity when subsequently injected into mice [24]. In addition, muscle tissue maturation is found to be highly stiffness-dependent [25–27]. Myosin/actin striation is observed when C2C12 cells and human myoblasts are cultured on substrates with physiological stiffness, which is indicative of improved tissue maturation.

2.1.4. Multi-cellular environment

Satellite cells make up approximately 2–7% of the total nuclear content of skeletal muscle. They locate between the basal lamina and the plasma membrane that surrounds each fiber, and function as putative stem cells in skeletal muscle. These cells are quiescent in mature, healthy tissues and are specified by expression of paired box 7 (Pax7) [12]. Satellite cells play a pivotal role in muscle fiber repair. They react upon injuries, switching from quiescent to active. Satellite cells migrate to the injured site, proliferate, undergo myogenic differentiation, fuse to form new myofibers, and integrate with the muscle. Seminal studies have demonstrated the efficacy of satellite cell transplantation [28,29]. The transplantation of single intact myofiber with seven satellite cells into radiation-ablated muscles produced over a hundred new muscle fibers with thousands of nucleus [28]. Robust self-renewal and expansion have been observed. Given the myogenic potential, satellite cell is a suitable source for muscle regeneration. However, they are highly heterogeneous in function and thus with varied efficacy in regeneration [8,28,30–32]. Moreover, the difficulty in isolation and purification of the cells and the low expansion capacity *ex vivo* is yet to be addressed [8,33]. This has greatly intrigued the interest in exploring various cell types with comparable regeneration capability. Myoblasts [34], mesoangioblasts [27,35], pericytes [36,37], embryonic stem cells (ESCs) [38], induced pluripotent stem cells (iPSCs) [39], mesenchymal stem cells (MSCs) [40,41], muscle-derived stem cells (MDSC) and adipose-derived stem cells (ADSCs) have been extensively evaluated for their myogenic capability [42,43]. Some detailed reviews have summarized the cell sources and types for skeletal muscle regeneration [44,45].

Muscle contraction is regulated by the intimate collaboration of muscle tissue, capillaries, nervous tissues, and connective tissues. Hence, it is necessary to bring together muscle cells, fibroblasts, neurons, and endothelial cells when constructing *in vitro* muscle tissues. The interaction between muscle cells and fibroblasts is essential as the ECM proteins and some growth factors are mainly secreted by interstitial fibroblasts. Cooper et al. have clarified the possible role of fibroblast as an elastic substratum to support contractility and maturation [46]. Specifically, cells cultured on collagen- or laminin-coated substrates detached massively after 5–6 days differentiation, whereas for C2C12 cultured on fibroblast substratum, extended contractile myotube culture period has been observed. The highly mature sarcomeric structure was confirmed by immunostaining. Electrical stimulation at 10V was applied and the occurred reproducible calcium transients revealed the functional maturation in terms of calcium handling proteins. A growing body of studies has further confirmed the potential of fibroblasts on promoting the C2C12 differentiation and stabilizing the tissue integrity [47–50]. In a recently published study, Rao et al. conducted a co-delivery of myoblasts and fibroblasts using decellularized skeletal muscle extracellular matrix (SkECM) hydrogel to tibialis anterior (TA) mice models [49]. Myoblasts alone or co-delivery with PBS was run as a control. The skECM with fibroblasts has exhibited increased cell viability and better perfusion in comparison to the saline group. It is noteworthy that co-delivery with a better recapitulation of the native environment yielded more desirable results.

Skeletal muscle is a highly vascularized tissue. Capillaries are interspersed in the muscle fibers to facilitate the nutrients/oxygen transportation and waste removal. For thick engineered tissues, the absence of vascular network frequently induces tissue necrosis in the central zone and finally leads to the failure of fully functional recovery. To overcome this, myoblasts co-culture with endothelial cells to vascularize the tissue has been widely investigated [51–56]. Notably, Levenberg et al. reported a tri-culture by seeding myoblast, embryonic fibroblast, and endothelial cells (ECs) on highly porous scaffold (PLGA-PLLA) [53].

To analyze the therapeutic potential, the constructs were implanted into three different models. Continuous cell differentiation *in vivo* and host integration were observed in all three models. The quantitative analysis of the perfused vessels revealed that constructs with muscle cells only have 21 ± 2 vessels, while 30 ± 2 vessels were observed in the presence of endothelial cells. In a lateral study, Koffler et al. conducted the tri-culture on a biodegradable, acellular scaffold to analyze the degree of *in vitro* vascularization [56]. The constructs were cultured *in vitro* and observed at different incubation periods (1 day, 1, 2, and 3 weeks). ECs and myoblasts spread toward the perimeter of the scaffold within one day of culture. The vessel-like structure appeared at the peripheral of scaffold 1 week in culture. Two and three weeks later, the open vessel-like structures were observed at the center of the scaffold and almost covered the entire construct. The constructs with varied maturity (1 day, 1, 2, and 3 weeks) were then transplanted to the abdominal wall of nude mice to investigate tissue integration. Muscle formation was observed in all the groups, and increase with incubation time, fibers tend to be more organized and closely packed. This technology was further extended and applied to repair large soft tissue defects [55]. The triple-cultured constructs were cultured *in vitro* to form the small capillary networks and then implanted to the femoral artery and veins for prevascularization for 1 week. The extensive vascular density and perfusion indicated that the scaffolds were highly vascularized, therefore was transferred to abdominal viscera for a full-thickness abdominal wall repair. The engineered constructs remained viable, vascularized, and integrated well with the surrounding tissues. The tri-culture system has greatly enhanced muscle regeneration, maturation, and integration in comparison to constructs with a single cell type.

Muscle contraction begins when the nervous system generates an electrical signal, which is known as an action potential, travels through the motor neuron. The neuromuscular junction is where the motor neuron reaches a muscle cell. When the signal reaches the neuromuscular junction, motor neurons release a neurotransmitter called acetylcholine (ACh), which binds to the receptors on the outside of the muscle fiber. That initiates a chemical reaction within the muscle, causing muscle contraction. Given that neuronal input is crucial for muscles, electrical stimulation is frequently used to mimic the neuronal stimulation to induce muscle contraction in a laboratory environment. However, the

electrical stimulation is not conducive for long-term culture, which makes the neural stimulation necessary when constructing the *in vitro* muscle tissues [57].

By co-culturing skeletal muscle construct with fetal nerve explants [58], Larkin et al. demonstrated that spontaneous contraction took place only in the co-culture constructs. The presence of ACh at the junctions between nerve extensions and the muscle constructs was confirmed with immunohistochemical labeling. Morimoto et al. generated 3D free-standing neuron-muscle constructs with highly aligned and matured muscle fibers from the co-culture of skeletal muscle fibers and motor neurons [59]. They have developed free-standing muscle fiber constructs with C2C12-laden matrigel, followed by mNSC differentiation on the muscle constructs. The neurospheres were in tight connection with the muscle fiber bundle. The acetylcholine receptors (AChRs) were formed at the connection between the muscle fibers and the neurons. Strikingly, with the chemical simulation of glutamic acid on motor neurons, the muscle-neuron constructs contracted synchronously with a contractile displacement (37.7 μm) larger than that of spontaneous contractions (0.9 μm). Taken together, the incorporation of neurons has greatly enhanced muscle contractility [60]. Similarly, the co-culture system was applied to a fibrin-based 3D matrix by Martin et al. [57]. Immunohistochemical analysis confirmed the uniaxial alignment myotube formation and the attachment of neurons to the fibrin gel. Immunostaining of Synaptic Vesicle Protein 2 (SV-2) and AChR suggested the presence of putative NMJ formation within the fibrin gel. With the electrical stimulation, constructs cultured for 18 days exhibited 145% greater twitch force and augmented by 143% tetanic force in comparison to the control group (with no neurons). Moreover, the co-cultured constructs showed more consistent striations (84.42% ± 7.85% of myotubes) than aneural constructs (13.9% ± 4.47%).

Overall, constructs with multiple cell types have shown enhanced myogenic potential, better resemblance to native muscle tissue and conferred some muscle functions in *in vivo* studies.

2.2. Effect of geometrical confinement on tissue engineering skeletal muscle

Skeletal muscle consists of a bunch of unidirectional nanofibrils where organization determines functionality. As demonstrated, myoblasts grow randomly in the absence of contact guidance and this is not conducive to generate contractile tissues [20,61,62]. Therefore, it is advantageous to design scaffolds with appropriate topographical support to align the muscle cells. Early studies have been focusing on the effects of various micro- or nano-scale surface topology and patterning on directing cell arrangement and attempt to screen out the optimum features [63–65].

A number of patterns such as groove/ridges/channels [20,66,67], holes [68], square, circle and diamond posts [64], cantilever [69] and continuous wavy micropatterns [70–72], with feature sizes spanning a wide range have been evaluated. Groove/ridge pattern with size up to 100 μm allows the myoblast alignment and elongation, but with limited effect on cell differentiation. An outstanding study has been conducted by Charest et al. [68]. They analyzed the primary and C2C12 myoblast alignment and differentiation by a series of micro-topological patterns, including groove/ridges and an array of holes, with various sizes (width or diameter) ranging from 5 to 75 μm and depth around 5.1 μm (Fig. 2a). Notably, cell alignment has been observed in all the groove patterns but selectively aligned along the rows of holes. The alignment is modulated by the groove width, better alignment was observed on the narrower groove width. Evidenced by sarcomeric myosin and AchR expression, cell density, and differentiation were not significantly affected by the topography (Fig. 2b). In addition, groove/ridge pattern in nanoscale facilitates myoblast alignment as well [73,74]. Clark et al. suggested that ultrafine gratings (130 nm wide grooves separated by 130 nm wide ridges and 210 nm deep) allows cell alignment, but inhibits myotube formation.

In addition, continuous wavy patterns and posts enable cell alignment as well. Lam et al. demonstrated that a wavy pattern with 6 μm periodicity gives rise to the most healthymyoblast and optimum alignment (as shown in Fig. 2c and d) [72]. Through the comparison between grooves with sharp edges and sinusoidal wavy patterns with round edges, Jiang et al. have declared the negligible role of sharp edges for eliciting contact guidance [75]. Besides linear patterns, surface roughness encompasses the capability to align myoblasts as well [71].

Similarly, surface patterning has been frequently utilized to impart surface topology as contact guidance by modifying material surface chemically or physically. ECM proteins such as collagen, fibronectin, and laminin are commonly used to induce cell adhesion and direct cell alignment [26,77–79]. Laminin-coated substrates were identified to be superior to fibronectin- and collagen-coated regarding myotube numbers, myotube length, and fusion index [77]. Besides, cell repulsive materials such as PEG and PEO-PPO are employed independently to confine the area for cell mobility or work with cell-adhesive protein synergistically [26].

Apart from ECM proteins, other multi-functional materials have been investigated. With femtosecond laser ablation (FLA) technique, Park et al. have introduced a conductive graphene oxide-incorporated polyacrylamide (GO-PAAm) hydrogel with line topography to mimic skeletal muscle tissues (Fig. 2e) [76]. The hydrogel was chemically reduced after FLA-patterning to enhance the conductivity, which was referred to as r(GO-PAAm). Through parametric study, FLA was able to generate line patterns (20 μm in width and 10 μm in depth) with varied line spacing (20, 50, and 80 μm) on GO-PAAm hydrogel. The immunofluorescence analysis showed that all the micropatterned hydrogels induced unidirectional cell organization (Fig. 2f). Hydrogel with line spacing at 50 μm and 80 μm showed higher fusion indices than non-patterned samples and 20 μm patterned ones. Particularly, the r(GO-PAAm) showed slightly higher fusion indices. Myotube aspect ratio was examined and exhibited similar trends to the fusion index. The results indicated the synergistic effects of conductivity and proper geometrical confinement on myogenic differentiation.

Taken together, these 2D features function as tools to identify the potential of physical cues to induce cell alignment, promote myotube maturation and massively contribute to our understanding of the mechanism of how cells sense their surrounding environment. However, cells only sense the substrate topology when they are in direct contact with the substrates.

2.3. Effect of mechanical stimuli on tissue engineering skeletal muscle

Apart from proper materials, cell types, and appropriate topologies, suitable stimulation such as mechanical, electrical stimulation or a combination plays a pivotal role in regulating the biology. Skeletal muscle is in charge of voluntary movement in the body and subjected to cyclic stretch and relaxation constantly [80]. A number of studies have demonstrated the pivotal role of mechanical stimulation on regulating skeletal muscle cell behavior (as shown in Table 1) [81–84], yet the underlying mechanisms are not completely understood. Pioneer study conducted by Vandenbergh et al. has revealed that embryonic chicken myoblasts on a collagen-coated substrate aligned parallel to the strain direction under a slowly increasing uniaxial strain rate 0.35 mm/h for 3 days [85]. Muscle hypertrophy, increased protein expression, and DNA content were observed. Thereafter, a vast majority of studies have been performed to optimize the strain parameters including direction, duration, and frequency to elicit a desirable cellular response (Table 1).

Ahmed et al. investigated the synergistic effects of geometrical confined surface and cyclic tensile strain (CTS) on myoblast behavior systematically [86]. Briefly, they configured six different kinds of substrates: homogeneous FN functionalized substrates (1 MPa) with or without the presence of CTS; substrates with 0° line pattern (30 μm wide parallel lines with 40 μm line spacing) in CTS-free state; and 0°,

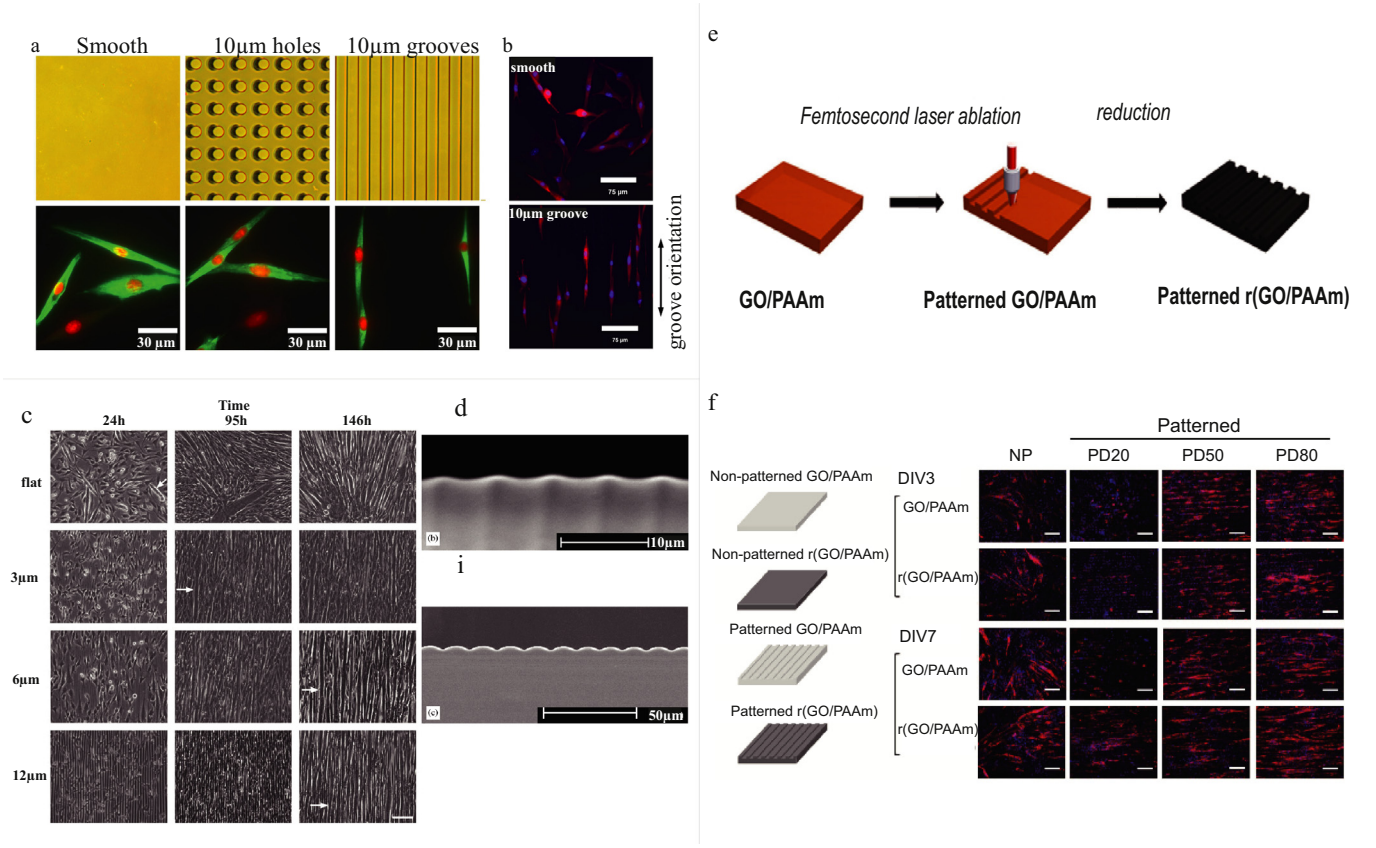

Fig. 2. 2D geometry confinement on skeletal muscle tissue engineering. a) Cellular orientation on various surface topologies, as evidenced by immunostaining of sarcomeric myosin and nuclei. b) AchR expression is not influenced by topography (Reproduced with permission from Ref. [68]. Copyright © 2007 Elsevier Ltd). c) Micrographs of muscle cells on different wave sizes. d) SEM images of 6 and 12 mm sized wavy PDMS substrate (Reproduced with permission from Ref. [72]. Copyright © 2006 Elsevier Ltd). e) Schematic of the fabrication process of the micropatterned r(GO/PAAm) hydrogel using femtosecond laser ablation (FLA) and chemical reduction. f) Immunostaining of C2C12 on micropatterned (GO/PAAm) *versus* r(GO/PAAm) and non-patterned hydrogels on d3 and d7 (Reproduced with permission from Ref. [76]. © 2019 Acta Materialia Inc).

45°. 90° micro-patterned substrates under CTS. Actin fiber orientation, nuclei aspect ratio, and nuclei orientation have been examined. For homogeneous patterned substrates, cells in strain-free conditions showed no specific orientation, and actin fibers extended to all directions randomly, while cells subjected to CTS tend to reorient their stress fibers around 71.5° to strain direction. In the micro-patterned surface under CTS, the stress fiber orientation is dependent on the line direction. In 0° patterned substrates, stress fibers were observed with 47.9° ± 19.5° relative to strain direction; in 45° lines, cells aligned roughly along the patterned lines; and in vertically patterned substrates, cells were highly elongated and aligned along the patterned lines. For nuclei orientation, nuclei elongated along with the direction of line pattern in all the micro-patterned substrates but randomly orientated in the homogeneous ones. This revealed that geometrical constraint is the dominant factor in nuclei orientation in comparison to CTS. Strikingly, striations were only observed in 45° patterned substrates. Given the difficulty of actin striation on stiff substrates, the results emphasized the importance of certain strain conditions on myogenesis could shield the negative effect of stiff substrates.

In a recently published study, Aguilar-Agon et al. have investigated the effect of mechanical loading on mediating skeletal muscle hypertrophy of 3D collagen-based skeletal muscle model using C2C12 cell line [81]. A continuous increasing load was applied to the engineered construct to achieve 15% stretch in 1 h, thereafter the construct was left under tension (15% stretch) for another 2 h. The mRNA expression of IGF-1, matrix metalloprotease 2 and 9 (MMP-2, 9), MuRF-1 and MAFbx after mechanical overload 0, 21, 45 h were examined. IGF-1 mRNA was significantly upregulated after 21 h and 45 h mechanical loading. Similarly, MMP-2 mRNA was observed with increased expression 21 h after loading. However, MMP-9 mRNA remained unaltered. A significant decrease in ubiquitin ligase MAFbx was detected 45 h after mechanical loading, while MuRF-1 mRNA expression remained relatively stable. The results of immunoblotting reported the increase in phosphorylation of Akt, p70S6K, and 4EBP-1 of the mechanically loaded scaffold. Besides, the increased myotube size and fusion indicated the myotube hypertrophy. Furthermore, the functionality of the muscle was assessed by measuring the tetanic force. The force production increased in a step-wise manner after 21 h (140%) and 45 h (265%) mechanical loading in comparison to the unloaded samples.

2.4. Effect of electrical stimuli on tissue engineering skeletal muscle

Neuronal stimulation is essential for skeletal muscle maturation and contraction. Using electrical pulse stimulation as a surrogate to elicit desired muscle contraction has been widely investigated. A growing body of research has been carried out to optimize the electrical stimuli (ES) protocol to better facilitate skeletal muscle activity and ameliorate muscle damage during the chronic stimulation period. A plethora of different ES protocols have been applied to 2D monolayer culture [87]. High-voltage stimulation (2–2.5 V/mm) or frequencies over 3 Hz was detrimental to C2C12 muscle cells in 2D planar culture [88]. A multitude of studies both 2D [89,90] and 3D [88,91,92] have demonstrated that electrical stimulation advances the differentiation and maturation of muscle cells, promotes force production [93].

An early study conducted by Brevet et al. reported that ES (14 h–48 h, 0.6 strain of 10- to 25-ms biphasic pulses delivered every 4 s for 7 h in total) rendered an increase in myosin accumulation and contractile protein synthesis in comparison to non-electrical stimulated control

Table 1
Overview of mechanical stimuli on skeletal muscle.

	Strain type	Materials	Cells	Amplitude, frequency, duration	Key feature	Reference
2D	Uniaxial stretch	Laminin collagen I proNectin coated membrane	MPC C2C12	0–2% (2d) followed by a uniaxial intermittent stretch regime of 2–6% (3 h on, 3 h off)	• No cell alignment • Maturation inhibited	[97]
	Uniaxial or equibiaxial CTS	Collagen I	C2C12	15%. 0.5 Hz, 1 s strain and 1 s rest for 48 h, then 3d rest	• Equibiaxial: no cell alignment; • Uniaxial: cell aligned perpendicular to the strain direction • Increased myoblast differentiation and myotube formation	[85]
	Equibiaxial stetch	Collagen-coated plates	C2C12	12%, 0.7 Hz, 1 h/d for 2d or 5d	• 2d: no significant change in myotube area and diameter • 5d: increase in myotube diameter and area (>2 fold)	[98]
	Uniaxial CTS	Silicone membrane precoated with collagen type I	ASCs	10%, 1 Hz for 24 h	• Cell alignment perpendicular to strain direction. • Compare to chemical treatment, mechanical factor has less effect on myogenic differentiation • The addition of mechanical stimuli upregulated MyoD, MyHC2, MyoG expression.	[98]
	Uniaxial CTS	Silicone sheets coated with fibronectin	Mouse BMSCs C2C12 Human gingival fibroblasts rBMSCs	10%, (0.08, 0.17, 0.33, and 0.50 Hz) up to 7d	• 0.17 Hz resulted good cell alignment • mBMSCs aligned parallel to strain vector while other cell types aligned perpendicular to strain direction • Upregulation of Myf5 and MRF4, myosin- and myogenin-positive myotube formation	[99]
2D	Uniaxial CTS	Collagen I coated substrate	Adipose-derived stem/stromal cell	11%, 0.5 Hz, 1 h/day, 18 days (from d3-d21)	• Cell aligned at almost 45° to the direction of strain • Increased expression of desmin, myoD and MHC	[100]
	Uniaxial CTS	Collagen-coated silicone rubber membranes	C2C12	20% elongation for 24 h 0.1 Hz 2 s on-time, 4 s off-time	• Decreased MyoD and MNF-a • No expression of myogenin and MNF-b	[100]
	Uniaxial CTS	Collagen-coated BioFlex plates	C2C12	17% strain, 1 Hz, 1 h of cyclic strain every 24 h for 5 days	• Enhanced proliferation • Inhibit differentiation into myotubes	[101]
	Uniaxial CTS	BioFlex plates	C2C12	10%, 0.25 Hz, 2 s strain and 2 s rest for 1 h/day for 5 days	• Cyclic stretch induces C2C12 proliferation • Inhibits MHC, MRFs expression and myotube formation	[102]
	Uniaxial CTS	Collagen-coated plates	Bovine satellite cells	10%, 0.25 Hz, 2 s strain and 2 s rest for 1 h/day for 5 days	• Induces the proliferation of bovine satellite cells • Suppresses their myogenic differentiation through the activation of ERK	[102]
	Uniaxial CTS	NCO-sP (EO-stat-PO) hydrogel, fibronectin	C2C12	7%, 0.5 Hz, for 4 days (24 h/day)	• Geometrical costraint result fiber alignment but no influence on proliferation or differentiation • Geometric constraint is the dominant factor in determining necleus shape and orientation	[86]
3D	Static strain	Collagen/Matrigel	Primary human skeletal muscle cells	3.5um/10 min (10d) to reach 10% strain then hold for 3d 5% strain (2d) 10% strain (2d) 15% strain (4d).	• Cell alignment due to internal longitudinal tension • Increased myofiber diameter by 12% and area percentage by 40%	[103]
	Cyclic strain	Collagen-based acellular tissue scaffolds	Primary human muscle precursor cells	10%, 3 times/min for the first 5 min of every hour from 5 days to 3 weeks	• Unidirectional orientation • Analysis of tissue constructs retrieved 1 to 4 weeks post-implantation showed that constructs generated tetanic and twitch contractile responses with a specific force of 1% and 10%	[104]
	Cyclic strain	Fibrin	MPC, C2C12	A 2-day uniaxial ramp stretch of 0–2%, followed by a uniaxial intermittent stretch regime of 2–6% dynamic stretch (3 h on, 3 h off)	• Maturation inhibited	[97]
	Static strain	Fibrin	C2C12	10% static strain for 6 h, 18 h rest at 3% static strain, 7 days	• Cell alignment • Enhanced muscle maturity	[84]
	Continuous strain	Fibrin	C2C12	25% and 50% strain	• Cell alignment under continuous strain	[105]
	Continuous strain	Collagen	C2C12	Continuous increasing load to 15% strain in 1 h and remained tension for 2 hs	• Increase expression in IGF1 and MMP-2, decrease in MAFbx • Increased myotube fusion and size, force production	[81]

group [94]. Langelaan et al. investigated the ES effects (4 V/cm,6 ms pulses at a frequency of 2 Hz) in 2D and 3D culture with C2C12 and muscle progenitor cells (MPCs) [95]. The remarkable difference in maturation level between the two cell types was identified by cross-striations and expression levels of mature myosin heavy chain (MHC) isoforms, indicated that MPCs constructs were more susceptible to ES.

A recent study published by Khodabukus et al. has evaluated the effects of electrical stimulation on human engineering muscle structure, function, and metabolism [96]. The model was electrically stimulated with intermittent stimulation at 1 Hz and 10 Hz after 1-week differentiation. Notably, the 7-day electrical stimulation significantly increased nuclei numbers, muscle bundle size, as well as glucose and fatty acid metabolic independent of frequency. Moreover, a 3-fold higher twitch and tetanic force were found with electrical stimulation in comparison to the non-stimulated controls. Strikingly, the specific force was increased to 19.3 mN/mm^2 (1 Hz), which yielded the highest value reported hitherto for human engineering tissues. Upregulation of several sarcomeric proteins including dystrophin, MHC, and sarcomeric α-actinin suggested the maturity of the myotubes, which is consistent with previous studies.

Taken together, these studies stressed the indispensable role of mechanical and electrical stimuli in promoting myogenesis and force production. However, the strain regimen of these external stimuli should be further researched.

3. Engineering *in vitro* skeletal muscle tissues

2D monolayer studies have greatly advanced our understanding of the muscle regeneration mechanism and helped to identify the influential parameters such as pattern size and shape on myogenesis. However, with the absence of cell-cell and cell-ECM interactions, cells in 2D culture are inadequate to reflect the 3D culture conditions. Given its deficiency in thickness and shape flexibility, it is challenging for direct clinical application, and it is impractical to achieve functional tissues from 2D culture. Moreover, the contractile function is measurable in 3D culture, whereas it is not very straightforward in 2D culture. Thus, recent studies experienced a dramatic paradigm shift from 2D to 3D platforms.

Numerous bioengineering strategies have been implemented to generate 3D *in vitro* skeletal muscle tissues with varied length scales, from micron to millimeter size. Here we review the state-of-the-art status of these bioengineering approaches in mimicking skeletal muscle tissues.

3.1. Electrospun fibers

By presenting the cells with micro- or nano-scale topological cues, aligned fibers enable the mimicking of native anisotropic structure to align myoblasts in a highly efficient manner, thus gain great attention for skeletal muscle regeneration [106–108]. Nanofibers are found to be superior in promoting myotube assembly to micropatterned substrates [109]. Several approaches such as drawing, phase separation, templating, self-assembly allow the production of nanofibrous scaffolds have been widely investigated [45,110]. Here, we confine our scope to electrospun fibers to review the status of *in vitro* skeletal muscle tissues.

The electrospinning technology has been well established and discussed in detail by several prominent reviews concerning fundamental principles, compatible materials, effects of influential processing parameters among other variables [111,112]. Fine adjustment over the flow rate, needle size, collector type and electric field allows the generation of fibers with varied size-scale (from nano- to micro-) and shapes including randomly oriented fiber mesh [113], tubes [114], arrays [115], and cylinders [116]. It is well acknowledged that aligned fibers are superior to randomly orientated ones in promoting cell alignment [117–119]. Both nano- and micro-scale fibers possess the capability to generate cell alignment [120]. This suggested that the dominant role of fiber orientation rather than fiber size over the cellular arrangement.

Both natural and synthetic polymers can be processed into fibers [113,121], collagen [122], chitosan [123], gelatin [124,125] and fibrin [51,126], silk fibroin [107,127], polycaprolactone (PCL), polylactic acid (PLA) and so forth have been electrospun independently or co-electrospun to generate fibrous scaffolds [123,128]. The incorporation of natural polymers greatly enhanced cell adhesion. In addition to co-electrospinning, surface coating was utilized to improve the biocompatibility with several ECM-proteins, such as gelatin [129,130], Matrigel [131], collagen [131,132], laminin [133] and fibronectin [109,131]. Zahari et al. electrospun PMMA nanofibers and coated with laminin or collagen, in the presence or absence of genipin [133]. A mixture of myoblasts and fibroblasts were seeded on the surface of the scaffold. The results demonstrated the remarkable myoblast proliferation and migration on the laminin-coated scaffold, while the collagen-coated surface was more supportive for fibroblasts. The results underscored the critical importance of the chemical environment for promoting cell attachment and proliferation.

As revealed by many researchers that electrical stimulation is conducive for promoting myotube formation and maturation, conductive materials such as carbon nanotubes [136], Poly(3,4-ethylene dioxythiophene) (PEDOT) [108,137], gold nanoparticles, graphene oxide (GO) [138], polyaniline [139], and silver nanoparticles are frequently incorporated to endow the scaffolds with conductivity [140–142]. Ku et al. have incorporated PANi into PCL polymer (200 mg/ml) to fabricate the conductive nanofibrous scaffold [134], and investigated the synergistic effects of topological and electrical cues on myoblast behavior. PANi with varied concentrations from 0 to 3 mg/ml was added and randomly oriented fibers were used as control (Fig. 3a). The results demonstrated that cellular organization has been steered by fiber orientation, and thus myotube direction, which is in good accordance with the previous research. Moreover, cell growth and proliferation were similar in all the groups, independent of fiber orientation and PANi concentration. While reflected by MHC expression and gene expression, fiber orientation, and PANi concentration have shown significant impact on myoblast differentiation (Fig. 3b). Chen et al. have also investigated the combined effects of topological guidance and electrical cues on myoblast behavior systematically [143]. The results added more evidence to the effectiveness of electrical cues on eliciting the desired cellular response.

A great deal of studies has reported the great potential of electrospun fibers on skeletal muscle regeneration. However, in most cases, densely packed fiber scaffolds lead to slow cell infiltration rate, which precludes the further application of the technology and render the fibrous scaffolds most likely to function as 2D surfaces. Several approaches have been introduced to address the cell migration issue inside fibrous scaffolds [126,144–146]. For instance, salted leaching [147], dual-polymer electrospinning with sacrificial materials [148] and cell electrospinning [135]. Yeo et al. fabricated the cell-laden nanofibrous bundle *via* cell electrospinning with alginate/PEO [135]. A single strut with 70–100 μm diameter and 30 mm length has been fabricated by cell printing and cell electrospinning. Weight fractions, processing parameters have been optimized to achieve an electrospinnable material and highly aligned structure with homogeneous cell distribution. In comparison to cell printing strategy, cell electrospinning has greatly improved the cell elongation, alignment, and differentiation. The result is in good agreement with previous findings that cells are compliant to nanofibers rather than micro-patterned features (Fig. 3c, d) [109].

Vascularization has been a long-standing challenge in engineered thick tissues. The absence of proper vascular networks would eventually lead to necrosis in the central part of the tissues. Gilbert et al. generated electrospun fibrin scaffolds with 15% alginate owing to its similar stiffness to native tissue and functioned as a sacrificial polymer to induce porosity for better cell infiltration [51]. Two types of scaffolds include "spread" and "bulk" were prepared. C2C12 was used to examine the *in vitro* performance of the scaffolds. Notably, in both types, densely aligned MHC^{+} myotubes, multinucleation, and sarcomeric striations were confirmed with immunostaining. Meanwhile, the spontaneous contraction was also observed. The C2C12-seeded scaffolds were subsequently transplanted into TA muscle defects in mice for 2 or 4 weeks. After 2 weeks, both bulk and spread scaffolds yielded significant regeneration, evidenced by the densely populated MHC^{+} myofibers and abundant network at the graft area. Myofiber density experienced a dramatic increase while capillary network density remained steady. Myofiber showed an average diameter of 23 μm, which is roughly half of the native myofiber. To better serve large muscle defects, the prevascularized scaffolds were prepared by co-cultured human endothelial cells and human adipose-derived stem cells on the C2C12-seeded scaffolds for 11 days. The scaffolds were therefore transplanted into VML defects and harvested after 10 days. Notably, as demonstrated by Ms-CD31 and DAPI, implanted electrospun scaffolds successfully anastomosed with host vessels and exhibited perfusion by host red blood cells (Fig. 3e).

Mounting evidence has confirmed the capability of electrospun fibers on modulating cell organization. However, cell infiltration into the dense fiber bundles remains challenging. The reported penetration depths are still limited to a few hundred microns, which is inadequate for thick tissues. In addition, electrospun fibers are not very straightforward in building 3D structures, not even complex anatomical structures,

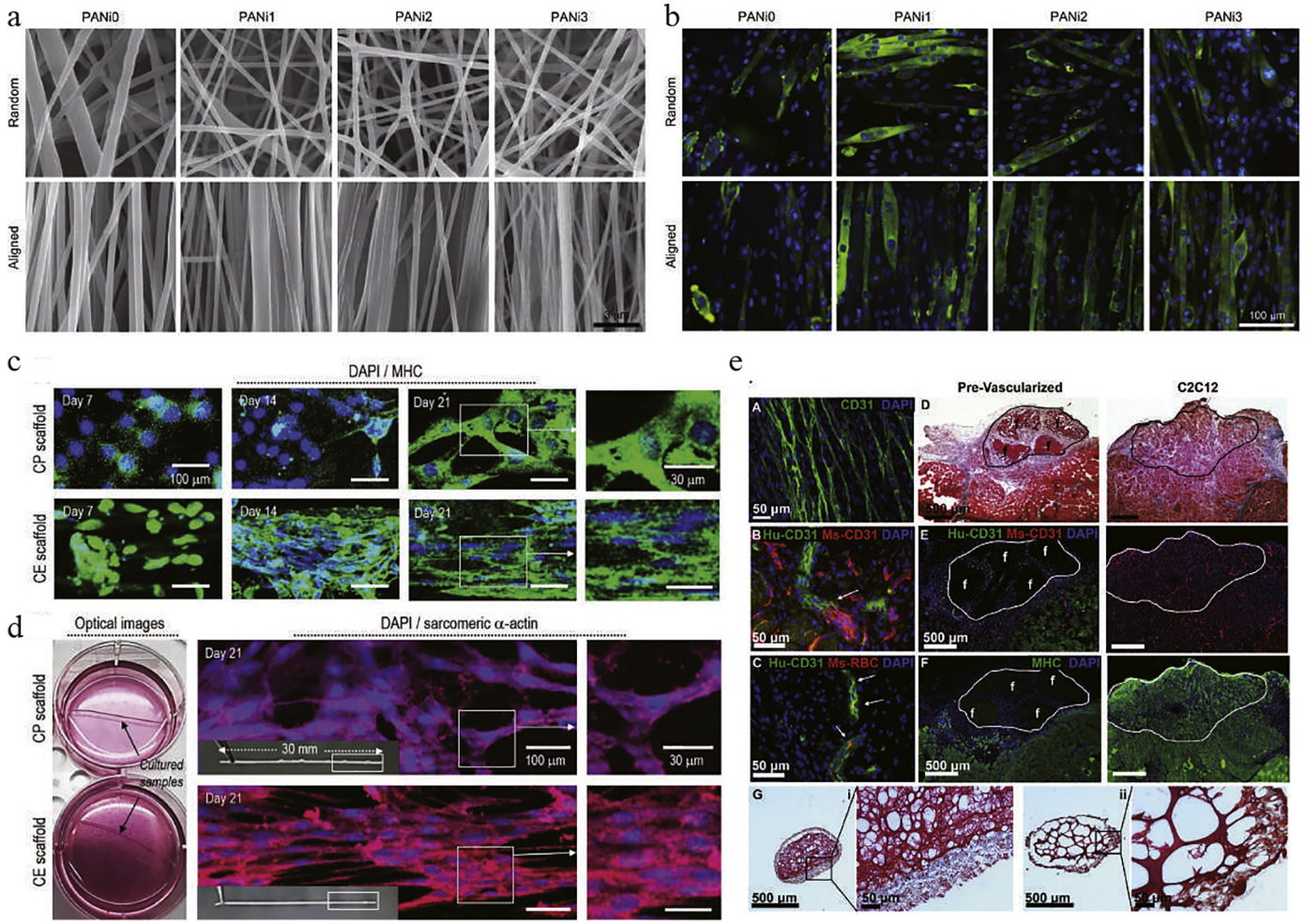

Fig. 3. Electrospun fibers for skeletal muscle regeneration. a) SEM images of PCL/PANi nanofibers with varied PANi concentration. b) MHC immunofluorescence staining of PCL/PANi nanofibers with varied PANi concentration (Reprinted with permission from Ref. [134]. Copyright © 2012 Elsevier Ltd). c) DAPI/MHC staining of cell electrospinning and cell printing samples at day 7, 14, and 21. d) Optical and DAPI/sarcomeric α-actin staining images after 21 d of culture (Reproduced with permission from Ref. [135]. Copyright © WILEY-VCH Verlag GmbH & Co. KGaA, Weinheim e) Immunostaining of pre-vascularized scaffolds in VML defect (Reproduced with permission from Ref. [51]. Copyright © 2018 Elsevier Ltd).

although near-field electrospinning or electrohydrodynamic printing have been explored for fabrication of 3D structures.

3.2. Porous hydrogel

In order to maximize the potential therapeutic effects of cells, a proper matrix for cell delivery is appealing. An engineered matrix is supposed to locate the cells to the injury site and improve the cell retention, offer instructive cues to enhance integration with host tissues, promote myogenesis, angiogenesis and neurogenesis, and degrade in a controlled manner to allow the new tissue ingrowth [149]. Owing to their high water content, biocompatibility, tunable chemical and mechanical properties, hydrogels have been widely explored for regenerative medicine and tissue engineering applications [150]. Numerous materials such as dECM hydrogel [9,49,151,152], collagen [81,153,154], gelatin methacrylol(gelMA) [25,155], chitosan-based [156,157], hyaluronic acid (HA) [158], fibrin [39,42,159], PEG-based [160,161], keratin [162,163], have been investigated (as listed in Table 2).

Although hydrogels exhibited great potential in tissue engineering applications, the disorganized and isotropic network structure is not conducive to cell alignment. Basically, hydrogels are applied to skeletal muscle engineering in three different forms: 1) micropatterning as geometrical confinement [173,188], 2) microstructures (unidirectional channels) in the hydrogels, 3) hydrogel scaffolds assisted with external stimuli to elicit a desired cellular response and cellular arrangement. Plenty of strategies have been employed to form biomimetic fascicle-like structures with hydrogels resembling that of native muscle tissue. Anchoring is broadly used. By applying passive tension on the hydrogel scaffold, myoblasts within the 3D matrix are promoted to fuse into multinucleated myotubes, ultimately form a uniaxially, aligned fiber bundles [34,92,189]. In addition, dynamic mechanical stimulation [81], magnetic stimulation [187] are recognized to be effective in facilitating myoblast alignment within the hydrogel.

3.2.1. 3D geometrical confinement

Through precise control over geometry, Aubin et al. have generated 3D cell alignment within GelMA hydrogel [188]. NIH 3T3-laden GelMA (5%) solution was micropatterned onto PEG-coated glass slides and followed by UV crosslinking for 20s, resulting micropatterned GelMA hydrogel with a thickness of 150 μm and varied width from 50 μm to 200 μm. Consistent with previous findings, the narrower width produces better cell alignment. To better assess the influence of cell types, they further extended the study to C2C12, HUVEC, and rodent cardiac side population cells (CSP), all of which form aligned, highly organized tissue *in vivo*. Human liver carcinoma cells (Hep-G2), which do not form unidirectional organized tissue *in vivo*, were utilized as control. As revealed by F-actin staining, HUVEC, C2C12, and CSP aligned longitudinally to the patterned hydrogels, whereas Hep-G2 fail to organize into aligned constructs. The study suggested that given appropriate

Table 2
Hydrogels in skeletal muscle tissue engineering.

Materials	Cells	Key features	Reference
Alginate-based	C2C12	• Tunable mechanical property • Stiffness and stress relaxation behavior of the substrates affect the spreading and proliferation of myoblasts	[164]
	Primary myoblasts	• Cell remained round shape and ceased to proliferate	[165]
	Satellite cells	• Fast degradation • Slow rate of myogenic potential	[166]
dECM	Primary rat aortic smooth muscle cells and C2C12	• Injectable • Increased neovascularization • Increased infiltration of muscle cells	[152]
	C2C12, HUVEC, human skeletal muscle cells	• Biocompatible • Weak mechanical property	[151,167]
Fibrin-based	Primary myoblasts	• Max twitch force 329 ± 26.3 μN • Max tetanic force 805.8 ± 55 μN • IGF-I resulted in a 50% increse in force production	[92]
	Primary myoblasts	• Adherent cell fraction and dynamic culture • Total cross-sectional muscle area (~3-fold) • Myofiber size (~1.6-fold) • Myonuclei density (~1.2-fold), • Force generation (~9-fold) in comparison to static culture and traditional use of freshly isolated cells	[168]
	C2C12, hMPCs	• Multiple, progressive delivery of cells • Weak mechanical property • Improved cell viability and muscle regeneration	[169]
	Human muscle cells	• Cell delivered with fibrin microthreads • Promotion of in-growth of new muscle tissue • Reduced levels of collagen deposition	[170]
	Human myoblast	• Myoblasts actively stiffened the 3D fibrin • Elastic modulus of the gel further increased upon myotube differentiation	[171]
	Neonatal rat myoblast	• Material selection impact the contraction force • 2 mg/ml fibrin yielded isometric tetanus amplitude of 1.4 ± 0.3 mN as compared to 0.9 ± 0.4 mN measured in collagen I-based bundles.	[172]
	C2C12, primary myoblasts	• Engineered tissue with controlled size, thickness, porosity and the spatial distribution of cell alignment. • Cell-mediated gel compaction in Collagen is less significant then that in fibrin gel	[173]
	C2C12	• Cell alignment • Enhanced muscle maturity	[84]
	Human muscle progenitor cells, HUVEC	• Human Bioartificial muscle model containing endothelial cell networks	[174]
Collagen-based	C2C12	• Mechancial loading • Increase expression in IGF1 and MMP-2, decrease in MAFbx • Increased myotube fusion and size, force production	[81]
	Primary rat muscle cells	• Significant proliferation in collagen-I-fibrin matrices and collagen nanofibers in comparison to collagen sponge • Cell alignment in collagen nanofibers	[154]
Gelatin-based	H9c2 myoblasts	• Gelatin bubble-based scaffold with a honeycomb-like structure • Slower cell proliferation in comparison to 2D but higher myogenin messenger RNA level	[175]
	C2C12	• Compliant mechanical stiffness ~13 kPa • Surface topology for cell alignment	[176]
GelMA	C2C12	• Groove/ridge 100/50 and 100/100 μm • Smaller ridge yielded better myotube alignment • Electrical stimulation improved the myoblast alignment and increased the diameter of the myotubes	[25]
	C2C12	• Smaller cross-section yielded more closely packed myotubes • Stiffness 1–3 kPa support cell differentiation in 3D gel	[155]
	C2C12	• Co-culture C2C12/PC12 • With PC12, C2C12 showed improved differentiation, enhanced myotube formation. • Increased myotube alignment, length and coverage area • Upregulation of the mRNA expression of muscle differentiation markers, muscle maturation marker, neuromuscular marker	[177]
	C2C12	• Aligned carbon nanotubes within GelMA hydrogels using dielectrophoresis • Higher conductivity, maturation and contractility in comparison to randomly distributed carbon nanotubes	[178,179]
	MuSC	• Substrate stiffness regulates cell behavior • Unlike rigid plastic dishes (~10^6 kPa), MuSC on softer substrate(12 kPa) self-renew *in vitro* and contribute extensively to muscle regeneration in subsequently transplantation	[24]
PEG-based	C2C12	• PEG-RGD hydrogel • Long channels: width (70–250 μm) and depth (100–240 μm) • Large features promote alignment in 3D, which do not readily facilitate cell alignment in 2D	[180]
	C2C12	• PEG hydrogel and electrospun fibers to present micro- and nano- features to promote cell alignment	[181]
	C2C12	• Elastic conductive poly(ethylene glycol)-*co*-poly(glycerol sebacate) (PEGS) grafted aniline pentamer (AP) copolymer promote the formation of myotubetunable • Tunable conductivity and mechanical properties by adjusting AP content	[182]
	C2C12	• (PEG)(5%w/v)-maleimide (MAL) functionalized with 2.0 mM RGD • Increased myoblast viability and differentiation,	[183]
	C2C12	• Hydrogel/fiber combinatorial system Core-shell structure to better induce cell alignment	[184]
	Pericytes	• PEG-fibrinogen hydrogel support adult pericytes and significantly improved their myogenic differentiation and angiogenic potentials *in vitro* and *in vivo*	[37]
	Mesoangioblasts	• PEG-fibrinogen hydrogel support Mesoangioblasts and significantly improved their myogenic differentiation	[185]
	SCs	• Synthetic hydrogel for cell delivery	[161]

Table 2 (*continued*)

Materials	Cells	Key features	Reference
		• Improved *in vivo* cell survival, proliferation, and engraftment in nonirradiated and immunocompetent muscles of aged and dystrophic mice	
HA-based	Primary myoblasts	• 3% HA functionalized with the laminin peptide, IKVAV enhance the myogenic behavior	[158]
	SCs, MPCs	• Preserved myogenic potential of SC • Major improvement in muscle structure and number of new myofibers with HA/SC in comparison to HA/MPC	[186]
Chitosan	C2C12	• 3D uniaxial tubular porous scaffolds • Comparable mechanical stiffness • Myotubes of ~50 μm diameter	[156]
	C2C12, HUVEC	• Self-healing and electrical conductive	[157]
POEGMA/CNC[a,b]	C2C12	• Rapid gelling • Noninvasive magnetic field stimulus • Improved myotube orientation	[187]
Keratin (KN)	MPCs	• Effective growth factor delivery • KN+bFGF+IGF-1 enabled a greater recovery of contractile force than KN+bFGF, KN+MPC, KN+MPC+bFGF+IGF-1, KN+IGF-1, KN+MPCs+bFGF	[162,163]

[a] POEGMA: Poly(oligoethylene glycol methacrylate).
[b] CNC: cellulose nanocrystals.

geometrical features, cells with the intrinsic potential to align *in vivo* will spontaneously form aligned, elongated constructs *in vitro*. With a larger geometry, Costantini et al. have investigated the influence of geometrical confinement and mechanical stiffness on the 3D GelMA hydrogels regarding myogenesis. Through varying the polymer concentration (3%, 4%, 6%, 8%) and crosslinking degree (4 min UV or 5 min UV), they have formulated a set of GelMA with varied mechanical properties ranging from 1 to 17 kPa. GelMA hydrogels with three different cross-sections: 2000 × 2000 μm, 1000 × 1000 μm, 500 × 500 μm were fabricated with PDMS mold and 2×10^7 cells/ml of C2C12 were encapsulated. The results revealed that cells underwent rapid spread at the lower concentration of GelMA (3%, 4%), while limited spreading was observed at higher concentrations (6%, 8%). In terms of geometry confinement, smaller cross-section resulted in better cell alignment and a more homogeneous myotube distribution. Cell-mediated gel compaction along with the decreased cross-section was observed in all the groups. The study underlined the crucial role of mechanical property and geometrical features in constructing 3D muscle tissues.

3.2.2. Hydrogels with unidirectional channels

Apart from the geometrical confinement, adjusting the microstructure of the hydrogel is a promising alternative to direct cell alignment. Thermally-induced phase separation followed by free-drying is an effective approach to creating anisotropic microporous scaffolds that enable myoblasts alignment and thus oriented myotube formation [156,190–193]. Leveraging on the directional freezing technique, Jana et al. have developed the 3D uniaxial tubular porous scaffolds made of chitosan [156]. Briefly, the chitosan solution was poured into a cylindrical Teflon mold which has a metal cap on one end and a Teflon cap on the other. During lyophilization, the Teflon cap was maintained at 25 °C, and the other was kept in low temperature to establish a temperature gradient that allows the formation of tubular porous microstructure within the scaffold. The effect of the polymer concentration (4, 6, 8, and 12 wt%) and freeze-drying temperature (metal cap temp: −20 °C, −70 °C and −180 °C) on the scaffold properties (structural and mechanical) were investigated. The results demonstrated that the pore sizes range from 200 to 500 μm, 30 to 250 μm, and 10 to 50 μm under −20 °C, −70 °C and −180 °C, respectively. A similar trend has been observed between pore size and polymer concentration. The pore size decreases with increasing polymer concentration. The mechanical property increased when increasing temperature gradients. Notably, polymer concentration had a significant effect on myotube diameter rather than myotube length. Taken together, the study has introduced a strategy to create unidirectional pores within the 3D matrix with tunable properties to facilitate the engineering of oriented tissues.

3.2.3. Hydrogels with external stimuli

Mechanical tension has been frequently utilized to facilitate myoblast alignment in 3D tissue engineered muscle models. Kim et al. [194] have revealed the significant role of PCL pillar printed along with the tissue in driving cell alignment since low cell density and disorganized structure has been observed in the tissue printed without PCL pillar. Using mechanical tension to induce cell alignment has been well established in many other studies. Huang et al. developed a self-organized myoblast-encapsulated 3D fibrin scaffold [92]. The fibrin gel was fixed with two silk sutures pinned at each end of the plate. Myoblasts were seeded and differentiated on top of the fibrin gel. Cell-mediated contraction of the gel culminates 10 days after plating. The contractility was measured after 14 days. The engineered tissue generated a maximum twitch force of 329 ± 26.3 μN and a maximal tetanic force of 805.8 ± 55 μN when electrically stimulated. Interestingly, the addition of IGF-I with the varied amount (25, 50, or 75 ng) in the fibrin gel resulted in 50, 36, and 31% increases in force production compared to untreated 3D tissue. Although the diameter of myotubes formed did not exceed 10 μm, the study has shed light on the development of *in vitro* 3D skeletal muscle tissue.

Gholobova et al. have generated endothelial networks within a fibrin-based bioartificial muscle (BAM) which has been discussed above [174]. In a recent study, they have applied the model to drug testing [34]. The engineered muscle was fabricated based on the well-established protocol by encapsulating C2C12 mouse myoblasts, human myoblasts, or human mixed muscle cells in fibrin gel in a silicone mold containing 2 attachment points respectively. The engineered tissues were maintained in growth medium for 2 days and subsequently switch to differentiation medium, and kept for 7 days before the injection. Multiple compounds including a dye (Trypan blue), a hydrolyzable compound CDFDA, a reducible substrate (pro-NanoLuc), and a wasp venom toxin (mastoparan) were selected. Direct reflux, release, and metabolism were characterized in BAM comparison to 2D cell culture and isolated human muscle strips. The authors started with the parameter optimization of the BAM (1 mg/ml fibrin with a thickness just below 2 mm) to enable up to 1 μl per injection site, the concentration of the injected compound to ensure they were detectable, and direct reflux when removing the needle with Trypan blue. Creatine kinase (CK) is an intracellular enzyme that releases upon cell damage. Mastoparan (1 μl, 1 mg/ml), a wasp venom peptide was injected once or four times to BAM. HBSS was injected as a control group. CK release in BAM was in a dose-dependent manner. With regard to CDFDA and pro-NanoLuc, 80% of CDFDA was released after 1.5 h, while only 40% of pro-NanoLuc release was detected. The disparate release profile between BAM and 2D cell culture has highlighted the benefits of the 3D BAM in drug release and toxicity testing.

In addition, taking advantage of shear force, shear-induced alignment is prevalent in injectable hydrogels. Injectable hydrogels are advantageous owing to the ease of manipulation, the good shape conformity to the defect site and minimally invasive and are very attractive in a controlled delivery. Utilizing pH-dependent collagen fibrillogenesis, Nakayama et al. introduced a nanofibrillar collagen scaffold with shear-based extrusion to form aligned fibrils [52]. SEM confirmed that the nanofibrils with a diameter range from 30 to 50 nm aligned along a uniaxial direction. C2C12 were cultured on both randomly oriented scaffolds and aligned scaffolds and went through a 5-day differentiation. Human endothelial cells were used for co-culture with the myotubes for another 4 days. As demonstrated by the immunostaining of MHC, the aligned scaffolds gave rise to the formation of longer myotubes in comparison to the randomly oriented scaffolds. Notably, the average length of myotubes was further promoted from 510 ± 60 μm to 760 ± 10 μm in the presence of endothelial cells. Additionally, the aligned endothelialized engineered scaffolds exhibited more striated myotubes than randomly oriented scaffolds. Notably, aligned endothelialized engineered scaffolds demonstrated greater contractile magnitudes and a more highly synchronized movement. Increased secretion of angiogenic and myogenic cytokines by endothelial cells was observed in engineered skeletal muscle formed from aligned scaffolds. To evaluate the therapeutic efficacy, the scaffolds were implanted into mice for regenerating TA muscle defects.

Similarly, the shear force has played a pivotal role in extrusion-based bioprinting technology. This will be discussed separately in the later sections.

3.3. Combinatorial effects of fibers and hydrogels

Fibers and hydrogel matrices have been broadly exploited individually to regenerate muscle tissue due to their ability to mimic the native tissue properties. However, the low cell infiltration rate in the fibrous scaffold and poor mechanical property of the hydrogel scaffold have yet to be addressed. With this in mind, 2-in-1 platforms comprising nano- and micro-scale features to guide cell alignment and reinforce the mechanical property simultaneously have been proposed [195,196]. The hybrid platforms could harness the strength of both fibers and hydrogels. Several configurations of fiber/hydrogel scaffolds have been delineated by [197]. Generally, laminated sandwich structures by stacking fiber sheets between hydrogel layers [198,199], or the core-shell structure by encapsulating fibers in hydrogels are most commonly used forms [184,200]. One simple study has been reported by Jana et al. [198]. They have introduced a laminated structure with chitosan scaffold bands placed on top of aligned chitosan/PCL nanofibers. The chitosan scaffold bandwidth is 20 μm, the spacing between two bands range from 50 to 100 μm. Fiber diameter lies between 100 and 150 nm. Over a 6-day culture, the control group with chitosan-PCL film substrate showed an unorganized cell distribution. Cells on pure nanofiber substrate have been reported with the highest alignment, while the chitosan scaffold bands on the chitosan-PCL aligned nanofibers group yielded better MHC expression. The results signified that the nano-scale feature is advantageous in promoting myoblast alignment and elongation, and the combination of nano- and micro-scale features induces late-stage myogenic maturation. A similar study was conducted by Cha et al. [181]. Bring together the PEG patterning and electrospinning technology, they have developed a dual-scale cell culture system which is composed of aligned PCL nanofiber sheet with the micro-patterned surface. The PEG hydrogel pattern was set at 100 and 200 μm with a fixed interval at 200 μm. The fiber substrates were fabricated with three different orientations: random, perpendicular, and parallel to the PEG line pattern. C2C12 cells were then seeded on the scaffold. Notably, on the perpendicularly oriented fibers, over 70% of cells were dispersed within $\pm 10°$ of the fiber orientation; while on the paralleled fiber substrate, over 90% cells were aligned to the fiber direction. The nuclei orientations were more likely to be affected by nanofiber direction, which confirmed that the nano-scale feature is dominant in comparison to the micro-scaled one. Further, MHC expression was quantitatively examined by the relative intensity of MHC expression against the cell number. On randomly oriented fiber substrates, the negligible difference of MHC expression was spotted between 200 μm and 100 μm. On patterned fibers, higher expression was observed on 100 μm than 200 μm, indicated the effect of geometrical confinement on myogenesis.

These studies have identified the specific role of nano- and micro-scale features in modulating myogenesis and paved the way for 3D studies. Ling Wang et al. developed a 3D core-shell composite scaffold [184]. Specifically, the core-shell composite scaffolds, in which the aligned nanofiber PCL/SF/PANi yarn (NFY) core were ensheathed by poly(ethylene glycol)-*co*-poly(glycerol sebacate) (PEGS-M) hydrogel. By adjusting the drawing speed, a series of NFY with varied diameters (50, 100, 165 μm) have been fabricated. The PEGS-M hydrogel column possesses a diameter of 550 μm and stiffness around 11 ± 3 kPa. C2C12 cells were seeded on NFY for cell attachment for 24 h, then coated with the hydrogel. The results demonstrated significant cell attachment and elongation after 24 h, evidenced by the increased aspect ratio of cells from 5.8 on the NFY to 8.5 after a 2-day culture in the hydrogel. The results highlighted the synergistic effects of nano- and micro-features. To better recapitulate the native structures, the author has extended the core-shell structure with two orthogonal layers of parallel aligned NFYs encapsulated in the hydrogel sheet. As revealed by the optical images, cells fully filled the peripheral surfaces of these NFYs within the 3D hydrogel sheet over 3 days of culture. Taken together, the results suggested the feasibility and potential of constructing a 3D environment for directing cell alignment with core-shell scaffolds that encompass both nano- and micro-scale features.

Generally, taken together fibrous structure and water-enriched hydrogels, the fiber/hydrogel scaffolds endow the cells with topological cues and present a 3D cell favorable environment with improved mechanical property. The collective efforts of nano- and micro-scale features have greatly improved skeletal muscle tissue maturation. However, most of the studies made no reference to the cell infiltration problem which still remains to be one of the critical challenges of such culture systems.

3.4. Cell/growth factor delivery in skeletal muscle tissue engineering

A major stumbling block that hinders the development of cell delivery is that cells can hardly survive the harsh environment including the host immune response and the enzymatic process [149,227]. Besides cells, a cascade of growth factors and cytokines are recognized in regulating the different aspects of the muscle regeneration process [228]. The most effective regulating factors in the myogenic process are growth factor IGF-1 and angiogenic growth factor VEGF [229], they both have been reported to positively influence muscle generation [230–233]. HGF and FGF2 are shown to be potent angiogenic factors [234]. Borseli et al. have systematically investigated the interplay of VEGF and IGF1 within alginate hydrogels for ischemic muscle regeneration. [231]. Five different configurations including alginate hydrogel alone, alginate with VEGF or IGF1, or both and bolus delivery of VEGF and IGF1 (3 μg each) in PBS have been studied. VEGF was released in a sustained manner, while IGF with a smaller size released faster *in vitro*. The results revealed that alginate/VEGF and alginate/VEGF/IGF both increased muscle blood densities compare to untreated and the bolus injection, IGF delivery showed a moderate effect on vascularization in gracilis and negligible effect in tibialis. Moreover, alginate/VEGF and alginate/VEGF/IGF delivery resulted in 80% and 95% of tissue perfusion, respectively. The results suggested the crucial role of VEGF delivery from alginate on angiogenesis. IGF delivery exhibited moderate effect in this study, this may due to the burst release of IGF. The co-delivery of VEGF/IGF with alginate has shown a remarkable effect on muscle regeneration, angiogenesis, and functional recovery. Taken together, the

study stressed out the crucial role of instructive cues in steering muscle regeneration and provided profound insight into growth factors delivery to treat muscle damage. Along this line, the author has extended the research and incorporated satellite cells to create dual delivery of cell/bioactive molecules(VEGF/IGF) within alginate gels to a more severe ischemia injury [235]. Cells delivered within alginate showed more robust engraftment at 3 days post-treatment in comparison to bolus injection, accompanied by increase size and mass of regenerating muscles. The cell/growth factors group also exhibited enhanced angiogenesis and tissue perfusion, while reduced inflammation and fibrosis compared to other conditions. Notably, the increased contractile force suggested the great efficacy of the dual delivery of cells and growth factors could help to further ameliorate the muscle damage.

3.5. 3D bioprinted skeletal muscle tissue

3D bioprinting had rapidly developed into a flexible and versatile tool in recent years. Exquisite spatial control over materials, cells and exogenous signaling render 3D bioprinting particularly attractive to generate 3D *in vitro* hierarchical functional tissues [201]. Incorporating specific cell types, growth factors and permissive materials, 3D bioprinting has achieved some remarkable progress in cartilage [202], eye [203], bone [204], cardiac [205], nerve [206], vascular networks [207,208], and muscles [209,210], in terms of structural heterogeneity and multi-cellular environment.

3D bioprinting allows the precise arrangement of cells, materials and functional molecules at the desired place in a pre-designed structure, and thus enables the construction of reproducible and scalable heterogeneous tissues which could possibly recapitulate the complexity of native tissues. The frequently used extrusion-, droplet- and laser-based technologies have been reviewed by loads of experienced researchers [211,212]. Among all the techniques, extrusion-based bioprinting has been frequently employed due to the ease of manipulation, cost-effectiveness, and broad material choices.

The selection of bio-ink plays an instrumental role in bioprinting. Basically, the bio-ink is supposed to be a printable, biocompatible, mechanically compliant, and with a degradation rate that could match the speed of tissue growth [213,214]. Both natural and synthetic materials have been widely explored and adapted to meet the requirement of specific bioprinting technology. Herein, we thoroughly review the progress of bioprinted muscle tissues in terms of materials, cells, structures, and functional recovery (Table 3).

Choi et al. have developed a skeletal muscle tissue model using dECM-based bio-ink with bioprinting to control the cellular organization [151]. PCL was deposited at the end of the constructs as geometrical constraints, applying passive tension to the cells within the constructs. Cellular orientation was analyzed with varied linewidth (500 μm, 1500 μm, 5000 μm). The results demonstrated that linewidth of 500 μm yielded the best cellular alignment and cell alignment was significantly increased over time (as shown in Fig. 4a). Particularly, cells were initially randomly organized in the linewidth of 5000 μm, while nearly 60% cells were elongated and aligned after 7-d differentiation (Fig. 4b). In comparison to collagen constructs, a higher-level expression of *Myo5*, *MyoG*, *MyoD*, and *MHC* was detected in dECM-based bio-ink printed constructs. Moreover, striation spotted in dECM-based constructs was indicative of the maturation of the constructs. Notably, Agrin, which is a functional ECM molecule participating in NMJ development, was detected in dECM bio-ink, gave rise to a remarkable number of α-BTX$^+$ cells in dECM-based bio-ink printed constructs. Together with the bioprinting presented topological cues, the dECM bio-ink may be advantageous in promoting skeletal muscle regeneration.

Given the outstanding performance of dECM bio-ink, the authors have further evaluated the therapeutic effect on the VML model in a recently published study [167]. The skeletal muscle dECM (mdECM) and vascular dECM (vdECM) bio-inks were derived from porcine tibialis anterior (TA) muscle muscles and descending aortas, respectively. Due to the low viscosity and weak mechanical property of the dECM bio-ink, gelatin granule-based (181.21 ± 73.38 μm) printing reservoir was used as supporting bath and as sacrificial materials to generate microchannels. PVA was added into the gelatin granules as a coagent to rapidly polymerize the dECM bio-ink to facilitate 3D stacking. A well-organized 3D skeletal muscle tissue in a dimension of 15 × 6 × 4 mm using human skeletal muscle cells was printed. dECM sponge and bulk dECM hydrogel with the same dimension were prepared in parallel as a control. *In vitro* study with pimonidazole showed that significant hypoxia occurred in bulk dECM hydrogel. The three types of constructs were then implanted into VML (40%) mice models for regeneration capacity assessment. The 3D printed constructed yielded 71% recovery compared to uninjured tissue. In order to maximize the therapeutic efficacy, vdECM bio-ink and HUVECs were incorporated to fabricate the prevascularized muscle constructs (Fig. 4c). The two different cell-laden bio-inks were deposited simultaneously with a coaxial nozzle to create a core-shell structure as shown in Fig. 4c. MHC and CD31 confirmed the formation of myotubes and endothelial networks. Specifically, in co-axial printing, myotubes were present inside and endothelial networks were surrounded in the outer layer, indicating the compartmentalized constructs were achieved (Fig. 4d). H&E staining of the constructs retrieved from VML models demonstrated the reduced fibrosis in co-axial printed constructs. MHC staining showed that the densely packed muscle fibers were more extensively distributed in the coaxial printing group in comparison to others (Fig. 4e). Furthermore, in the coaxial printed group, a remarkable higher number of co-localized hCD31$^+$ and mCD31$^+$ structures were observed, implying anastomoses with host vasculatures (Fig. 4f). *In situ* force measurement indicated 85% recovery in coaxial printed constructs. Taken together, the results suggested that by presenting spatially inductive cues, printing with dECM bio-ink could promote *de novo* muscle formation and functional recovery.

Merceron et al. engineered a muscle-tendon unit with integrated organ printing (IOP) technology [217]. A customized bio-ink consists of hyaluronic acid, gelatin, and fibrinogen were used to encapsulating cells (C2C12 and NIH/3T3). Thermoplastic PU and PCL were printed as the scaffolding of muscle-side and tendon side, respectively, with a 10% overlap to create an interface. C2C12-laden bio-inks were deposited within the gap of PU and NIH/3T3-laden bio-inks were localized within the gap of PCL, the printed construct (20 mm × 5 mm × 1 mm) was further crosslinked using thrombin for 30 min. The mechanical characterization revealed that the PU side with elastic modulus 0.39±0.05 MPa is more like elastomeric materials, while the PCL side with young modulus 46.67±2.67 MPa is much stiffer. The cells were able to survive the printing process and exhibited overall viability over 80% after 1-day culture. After 7 days, the cell viability slightly increased. Notably, C2C12 aligned anisotropically and expressed desmin and MHC, indicating their differentiation into myotubes. On the tendon side, collagen type I deposition was detected. This study has demonstrated the versatility of the IOP system and the feasibility of constructing tissues with heterogeneous properties. With this IOP system, Kang et al. have generated 3D anisotropic muscle tissue constructs (15 mm × 5 mm × 1 mm) [218]. PCL *pillars are printed as* scaffolding. C2C12 cells were printed with bio-ink consists of gelatin, fibrinogen, HA, and glycerol. Pluoronic 127 was deposited as support and sacrificial material. After crosslinking with thrombin, the uncrosslinked components including gelatin, HA, glycerol and Pluronic were washed away. As demonstrated by MHC expression, myotubes formation was observed after 7-d differentiation. To further evaluate the muscle tissue development, the 7-d differentiated constructs were implanted in nude rats subcutaneously, with a common peroneal nerve embedded to promote integration. Well-organized muscle fibers were observed in the retrieved constructs after 2 weeks. The presence of AChR clusters was confirmed by immunostaining of MHC and α-BTX. The double staining of α-BTX and neurofilament (NF) demonstrated the nerve integration *in vivo*. vWF expression revealed the vascularization throughout the constructs. Electromyography was performed to

Table 3
Overview of 3D printed skeletal muscle.

Printing strategy	Material	Cell	Printing parameter	Structure	Size	Mechanical property	Key feature	Reference
Extrusion-based	MdECM PCL constraints	C2C12	Printing T: 18 °C	Parallel type diamond type chain type	Filament width 500, 1500, 5000 μm	12 ± 3 kPa	• dECM bioink and 3D printing enable the mimicking of functional and structural properties of native muscle	[151]
Extrusion-based	MdECM VdECM PCL constraints Gelatin Granule bath	HUVEC Human Skeletal Muscle Cell	Printing T: 18 °C	Fiber bundle	15×6×4 mm	\	• Prevascularization promotes muscle regeneration	[167]
Extrusion-based	CMCMA, alginate-MA	C2C12	Nozzle dia: 200 μm	Two layers	Height: 250 μm Filament width: 200 μm	GelMA-CMCMA: 1.96 ± 0.16 kPa GelMA-AlgMA: 5.53 ± 2.01 kPa	• Composite bioink with tunable mechanical property	[236]
IOP	Polyurethane PCL, HA, gelatin fibrinogen	C2C12	PCL: 200 μm PU: 300 μm	Lattice structure	L×W×H: 20×5×1 mm	PU-C2C12 0.39 ± 0.05 MPa; PCL-NIH/3 T3 46.67 ± 2.67 MPa; Interface 1.03 ± 0.14 MPa	• Integrated tissue constructs with region specific biological and mechanical characteristics	[217]
ITOP	Fibrinogen gelatin HA, glycerol, PCL pillar Pluronic F-127	C2C12	~400 μm width	Fiber bundle structure	L×W×H: 15×5×1 mm	\	• Nerve integration and vascularization throughout the construct was observed *in vivo*.	[218]
ITOP	Fibrin, gelatin	hMPCs	~400 μm width	Fiber bundle structure	L×W×H: 15×15×15 mm	\	• 82% Functional recovery of TA defect • Nerve integration and vascularization was observed *in vivo*.	[194]
ITOP	Fibrinogen gelatin HA, glycerol, PCL pillar Pluronic	hMPCs, hNSCs	~300 μm	Lattice structure	L×W×H: 10×7×3 mm	\	• Increased cell viability • 1.71 fold increase in MHC^{+} myotube density • Increased AchRs per HPF and NMJs per HPF • Nerve integration and vascularization was observed *in vivo*.	[219]
Microfluidic Printing co-axial needle	PEG-Fibrinogen, alginate	C2C12	Hydrogel fibers ~250 μm	Aligned hydrogel fibers	7 layers thickness ~350 μm	\	• Multi-cellular • Enable the printing of non-easily manipulated materials	[224]
Extrusion-based	PCL-Collagen coated	C2C12	Nozzle dia: 350 μm	Microfibril structure	4–30 μm	20 MPa	• Cell alignment	[223]
Three-axis printing system with a dispensing system	Collagen	C2C12 H9C2 MC3T3-E1 hASC	Nozzle dia: 150 μm Printing cartridge T: 25°C Working stage T: 37°C	Grid pattern	12×6×0.8 mm^3	\	• High degree of cell alignment and high myogenic gene expression	[216]
Extrusion-based	dECM-MA, PVA coated	C2C12	Nozzle dia: 150 μm	lattice structure with topological cues	8×2×1 mm^3	\	• High degree myotube formation • Increased gene expression	[226]
Extrusion-based	PCL alginate/PEO	C2C12	PCL nozzle dia: 400 μm Alginate/PEO: 150 μm	Grid pattern	PCL strut dia: ~400 μm Fiber dia: ~1 μm	43–48 MPa	• Hierarchical scaffold consists of topological cues to direct cell alignment	[220]
Extrusion-based	PCL collagen/PEO	C2C12	PCL nozzle dia: 180 μm Collagen/PEO: 150 μm	Aligned fibers with collagen/PEO printed on the top	10 mm×15 mm×90 μm PCL fibrous bundle dia: ~100 μm	\	• Scaffold with topological cues and protein to induce myotube formation	[215]
Extrusion-based; Electrospinning	PCL, PVA Collagen Alginate, PEO	C2C12 HUVEC	PCL nozzle dia: 350 μm PVA/collagen 180 μm	Electrspun HUVECs-laden Alg on the top of PCL and collagen struts, C2C12 seeded on the vascularized structure	30 mm struts PCL (d: 298 ± 7 μm) PVA-leached PCL (286 ± 12 μm) PVA-leached collagen (286 ± 5 μm)	\	• High viability of HUVECs • High degree of the MHC with striated patterns • Enhanced	[222]

Table 3 (*continued*)

Printing strategy	Material	Cell	Printing parameter	Structure	Size	Mechanical property	Key feature	Reference
Extrusion-based	PCL	C2C12	PCL nozzle dia: 300 μm	Grid pattern	9mm×3mm×0.2 mm struct dia: 263.7 ± 6.7 μm	\	myogenic-specific gene expressions • Uni-axially aligned patterns on the surface of 3D printed PCL scaffold achieved by stretching • Myoblast alignment	[221]
Inkjet-printing	Suspension of C2C12 cells in sterile PBS solution	C2C12	dia: 85 μm	Cantilever	800×100×5 μm	\	• High resolution • Myotube formation	[237]
FDM with surface coating	Printing: PVA coating: PLA, agarose, SOEA	hMSCs	Nozzle dia: 300 μm	Cantilever	Layer height: 200, 100, 50 μm	\	• Staircase morphology • Cell alignment	[237]
Extrusion-based	Tetramer self-assembling peptides CH-01 and CH-02	C2C12	Nozzle dia: 400 μm	Circle, square	Circle dia: 8 mm Square: 6×6 mm^2, 3 layers	\	• Cell alignment	[238,239]

assess muscle function. Compound muscle action potential was 3.6 mV, indicating that the muscle was responsive to electrical stimulation, yet still immature. To determine the therapeutic potential, Kim et al. used the IOP system to develop 3D muscle constructs with human primary muscle progenitor cells [194]. The 3D bioprinted constructs (up to 15 × 15 × 15 mm) composed of fibrin gel as bio-ink (Fig. 4h), PCL pillar as scaffolding, and gelatin as a sacrificial material to create microchannels with a diameter of 300–400 μm. The constructs were cultured for 1 day in growth medium and 9 days in differentiation medium. *In vitro* results showed that the printed constructs maintained high viability throughout the culture period, while cells in non-printed constructs (10 × 10 × 3 mm, 30 × 10^6 cells/ml) mostly died in 5 days. Scaffold maturation was confirmed by MHC expression. Double-immunostaining of α-sarcomeric actin (α-SA) and laminin confirmed the presence of cross-striated myofibers, implied the muscle contractile properties. To optimize the cell density in bioprinted constructs, bioprinted constructs with varied cell densities (10, 20, 30, and 50 × 10^6 cells/ml) were implanted subcutaneously in mice. H&E staining confirmed the presence of constructs for up to 4 weeks. The retrieved constructs were characterized by MHC and human leukocyte antigen A (HLA) expression. Double staining identified that tissue formation increased with increased cell density, but the negligible difference was found between 30 million and 50 million. As more cells will increase the oxygen and nutrient consumption, the result suggested that 30 × 10^6 cells/ml was the optimal cell density in bioprinted constructs. To determine the therapeutic potential, the bioprinted constructs with a dimension of 10 × 7 × 3.6 mm were further applied to TA muscle defects. Strikingly, muscle force was recovered by up to 82% of normal muscle force by 8 weeks. H&E analysis showed superior myofiber formation and organization in bioprinted group and double staining of MHC/HLA confirmed the new myofiber formation (Fig. 4i). As evidenced by vWF/α-smooth muscle actin staining, the bioprinted constructs were well-vascularized at 4 weeks. Furthermore, the result of triple-staining of NF/AChR/MHC and NF/AChR/HLA indicated the innervation of the constructs and the integration of the newly formed myofibers in the bioprinted constructs with the host nerve system (Fig. 4j). The study highlighted the potential of the bioprinted constructs with the cellular organization for skeletal muscle regeneration. However, the constructs failed to support the full restoration at 8-week post-implantation. To tackle this problem, the group has further incorporated human neural stem cells (hNSC) [219]. The co-culture of human muscle progenitor cells (hMPC) and hNSC have been optimized and the optimal ratio of 300:1 was identified. With the incorporation of neural cells, the co-culture constructs have been demonstrated with increase cell viability and a 1.71-fold increase in MHC^+ myotube density in comparison to the hMPC alone group. In addition, the quantitative study of AchRs per HPF and NMJs per HPF has revealed the improved innervation potential of the co-culture constructs. The constructs were implanted into the TA muscle defect rat model, nerve integration, and vascularization of the constructs were demonstrated and an accelerated restoration as well.

Topological cues presented by electrospun fibers have shown great efficacy in promoting cell alignment. Intrigued by this, Yeo et al. have integrated electrospinning and cell printing to fabricate hierarchical scaffolds with micro/nano features [220]. Through melt-plotting, PCL was printed into a grid pattern to provide physical support. An adapted electrospinning approach was subsequently used to generate aligned PCL micro/nanofibers (AF) onto the plotted struts. This was followed by depositing C2C12-encapsulated alginate/PEO bio-ink. PEO was used as leaching material to release cells and enable cell migration. Constructs with randomly oriented fibers (RF) and no fibers (NF) were taken as control. The constructs were rolled up to create 3D free-standing tissues and cultured for 7 days. The live/dead assay demonstrated that cells survived the printing process and remained high cell viability over 94% for all types of scaffolds. Over a 7-d culture, cell number in AF and RF scaffolds underwent a dramatic increase, which indicated the fibers within the scaffolds largely enhanced cell proliferation. MHC staining on day 3 and 7 demonstrated a better alignment, higher myotube number, and length in AF scaffolds in comparison to RF scaffolds. The higher gene expression level of MyoD, myogenin, and troponin T in AF scaffolds than the rest underscored the critical role of fiber alignment in promoting muscle maturation. Similar results were obtained in a later study, Yeo and Kim [215] generated microfibrous bundle structure with electrohydrodynamic (ETH) process and cell printing using myoblast-laden collagen bio-ink (Fig. 4l). 3D PCL fibrous structures were produced with ETH printing with wet electrospinning. The 3D fibrous bundle was then subjected to uniaxial stretch with varied stretching percentage (0, 20, 40, 60, 80, and 100%) to achieve anisotropic structures, thereafter C2C12-laden collagen/PEO bio-ink was deposited on the fibrous bundle. Similarly, PEO concentration (1, 2, and 3 wt%) was optimized to facilitate cell release, stable cell attachment, and maintain structural integrity. Three different configurations were designed: aligned, randomly oriented, collagen-coated. The results indicated similar viability in all the groups, but with varied differentiation. Reflected by MHC staining, cell alignment has been observed in both aligned scaffolds. Notably, more homogeneous cell proliferation was achieved on the collagen-coated scaffold. The results indicated that the combination of topological effect and the biochemical effect is of considerable benefit to promote muscle development and maturation [215,220–222].

Bioprinting allows the generation of 3D constructs with a good cellular organization due to the intrinsic strain imposed on the molecules or fibers when the bio-ink flows through the nozzle. However, the printed filament dimension mainly depends on the nozzle size with an average diameter of a hundred microns. To better recapitulate the native muscle structure, some other strategies such as microfluidics, material fibrillation, stretching were engaged to generate more authentic constructs [216,221,223,224]. Kim et al. have developed a micropatterned PCL

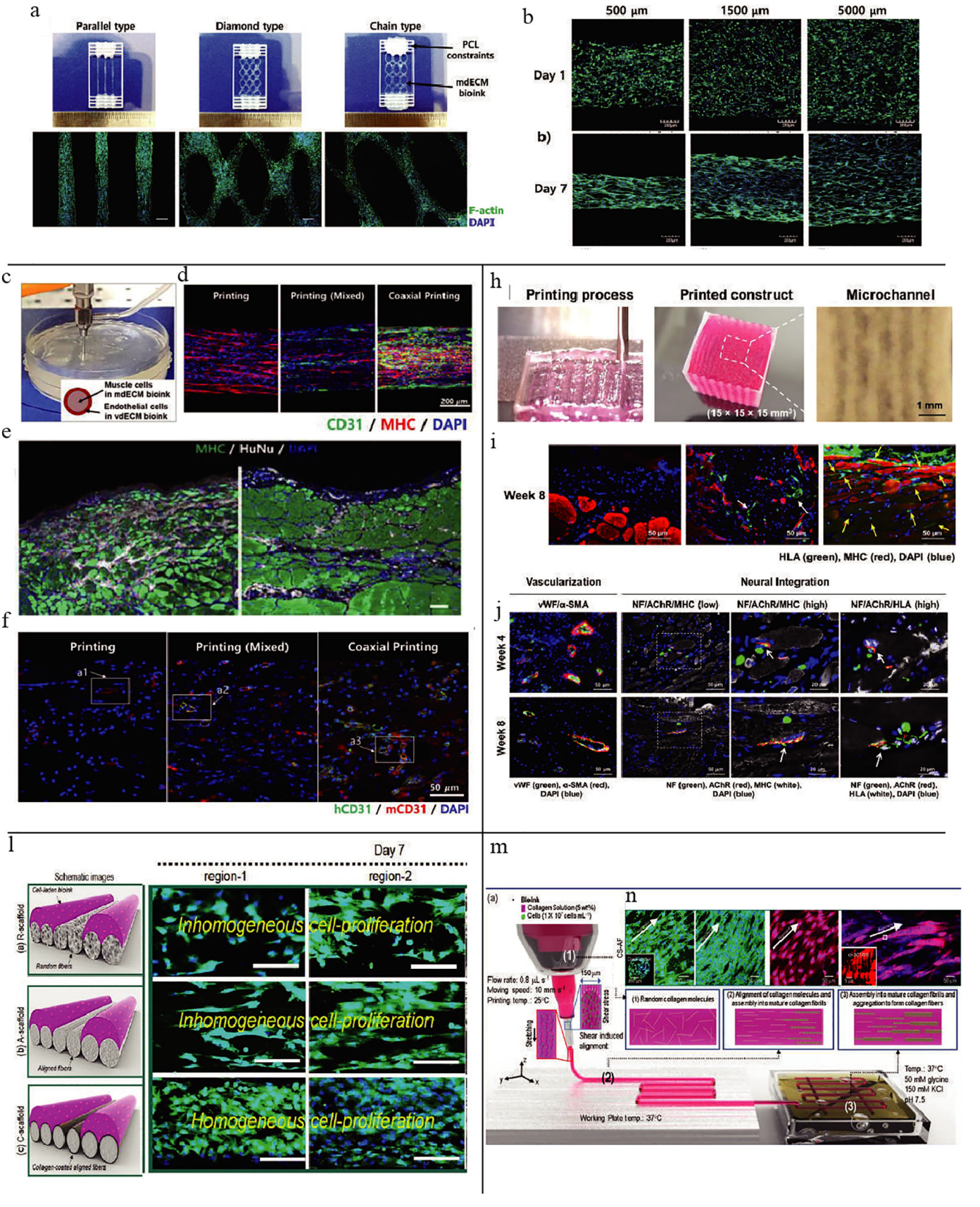

microfiber strut using the micro fibrillation/leaching process of PVA from a printed PCL/PVA structure [223]. Varied PCL/PVA ratio (1:9, 3:7, 5:5, 7:3, 9:1), processing temperature (70, 85, and 100 °C) and applied pneumatic pressure (150 kPa, 350 kPa) were examined in order to achieve fibrillated structure. Collagen-coating was employed to improve the bioactivity. Similarly, leveraging on collagen fibrillation, Kim's group has recently developed a microfibrous collagen construct through direct cell printing to induce orientation of collagen molecules, followed by collagen fibrillation to generate the topographical cue (Fig. 4m) [216]. Processing parameters including applied shear stress, moving speed, collagen weight fraction, and a fibrillating buffer solution (KCl and L-glycine) were optimized to produce a highly aligned cell-laden collagen structure without compromising cell viability. To determine the effect of surface topology on cellular activity, C2C12 cells were printed. Printed collagen constructs with the random surface pattern were used as control. MTT assay and live/dead staining showed similar cell proliferation rates and high cell survival rates in both groups. Phalloidin staining identified the unidirectional alignment in collagen constructs with surface topology, while no cell alignment was observed in the control group. As demonstrated by MHC and sarcomeric α-actinin staining and RT-PCR, the collagen structure with aligned morphology outperformed the unaligned collagen in terms of cell alignment, myotube formation, maturity and the level of myogenic gene expression (Fig. 4n). These could be due to the synergistic effect of topological cues and biochemical cues presented by collagen constructs. To further demonstrate the feasibility of this approach for various tissues, H9C2, hASCs, and MC3T3-E1 were investigated. Collagen fiber-induced alignment was demonstrated in all the groups. The results suggested that the technique of cell alignment using aligned collagen fibrils can be a new complementary method for regenerating various tissue systems.

Along this line, Kim et al. have produced a cell-laden dECM-based structure with specific topographical cues with the micro fibrillation/leaching process of PVA in a recently reported study. [225,226]. Briefly, the dECM hydrogel was prepared from the porcine skeletal muscle tissue, and a methacrylation process was performed to graft MA on dECM to achieve photo-crosslinkable dECM-MA. Further, the bio-ink was formulated by mixing 6% dECM-MA and 20% PVA in a 1:1 ratio. With C2C12 cells, structures with a dimension of $8 \times 2 \times 1$ mm^3 have been printed. With the combinatorial effect of biochemical and topological cues, cells in the printed constructs were observed with a high degree of myotube formation. In comparison to the control group (GelMA with topographical cues and dECM-based without topographical cues), approximately 1.5–1.8 fold of increased gene expression was detected in the printed dECM structure with topographical cues.

In comparison to conventional models, 3D bioprinting has apparently afforded higher freedom for the development of engineering skeletal muscle tissues. The controlled patterning of cells, materials, and biomolecular factors enables the generation of constructs with improved complexity and repeatability, that pave the foundation for personal medicine and high-throughput drug screening. Particularly, the collaborating with other fabrication technologies has further maximized the potential of 3D bioprinting.

4. Challenges and perspectives

Skeletal muscle tissue possesses extraordinary self-regeneration capability on minor injuries. However, the regeneration has been seriously impeded upon volumetric muscle loss. Unfortunately, the effective strategy enables the complete maturation and functional recovery of injured skeletal muscle is lacking. Hitherto, great efforts have been dedicated to exploring the mechanism behind skeletal muscle injury and the therapeutic potential by constructing *in vitro* engineered skeletal muscle tissues. Generally, recent progress in skeletal muscle tissue engineering has focused on the development of novel multi-functional biomaterials or mimicking the anisotropy of native structures, and thereafter, generates matured myotubes with comparative contractility to native tissues.

Plenty of strategies, both conventional approaches and bioprinting, have been implemented to induce anisotropic cellular arrangement by manipulating cells, materials, and instructive signaling to generate tissue models across varied length scales, from micron size to millimeter size.

In comparison to conventional methods, bioprinting is an appealing candidate in mimicking skeletal muscle tissues in an automated and controlled manner. Surprisingly, the collaborative efforts with microfluidic technology, spheroids, programmed control release and electrospinning has significantly enhanced the capability in capturing the key features of skeletal muscle tissues. Despite the great strides that has been made in bioprinted skeletal muscle models, it is still a daunting task to engineer a functional skeletal muscle tissue *in vitro*. To replicate the native muscle tissue more faithfully, the artificial construct is supposed to be comparative of native muscles structurally and functionally. The myotube diameter and contractile force are reported to be 50–100 μm and about 200 mN/mm^2, respectively. However, the myofiber size and contractile properties of *in vitro* constructs are still inferior to those of native adult muscle, which implies the incomplete muscle maturation. To better mimic the native skeletal muscle tissues, some of the limitations have to be addressed.

4.1. Immune response

Evidence of physiological studies has demonstrated that 3D *in vitro* constructs enable the regeneration of VML injuries to some extent. However, currently, the animal models in use are mostly immunodeficient or immunocompromised, which are inadequate to reflect the harsh physiological environment. The communication between the implanted model and the host is still not fully understood yet. More studies on immune response and inflammatory should be conducted.

4.2. Multicellular environment and cell source selection

Skeletal muscle tissue consists of several support cells including but not limited to fibroblast, vascular endothelial cells (ECs), and motor neurons, which enable blood flow and innervation of the tissue. Therefore, it is highly desirable to incorporate multiple cell types in order to capture the cell-cell interactions *in vivo*. Nevertheless, it is challenging to co-culture and differentiate multiple cell types as each cell type requires similar but different surrounding environments and culture

Fig. 4. 3D bioprinting in skeletal muscle tissue engineering. a) 3D printing of dsECM bio-ink to promote myoblast alignment. b) Cellular orientation in muscle construct with varied linewidth on day 1 and day 7 (Reprinted with permission from Ref. [151]. *copyright* WILEY-VCH Verlag GmbH & Co. KGaA, Weinheim). c) 3D cell printed prevascularized muscle construct with dsECM and dvECM bio-ink through co-axial printing. d) Immunostaining of different muscle constructs. e) Immunostaining of prevascularized constructs retrieved from VML injured TA muscle model. f) Immunostaining showing the vascularization of TA muscles treated with different muscle constructs (Reprinted with permission from Ref. [167]. *copyright* 2019 Elsevier Ltd). h) The bioprinted constructs with dimension up to 15 × 15 × 15 mm printed with ITOP system. i) Double immunofluorescence analysis of bioprinted muscle constructs on newly formed muscle. j) Immunofluorescence of vascularization and neural integration of the implanted constructs (Reprinted with permission from Ref. [194]. *copyright* 2018, Springer Nature). l. Microfibrous Bundle Structure Fabricated Using an Electric Field-Assisted/Cell Printing. (Adapted with permission [215]. *copyright*2018 American Chemical Society). m) 3D cell printing process using the Gly/KCl buffer solution. n) Immunofluorescence staining of DAPI (blue)/MHC (green) after 7, 14 and DAPI(blue)/sarcomeric α-actinin (red) images after 14 and 21 days of cell culture. (Adapted with permission [216]. *copyright* 2019 Elsevier B.V.).

mediums. Besides, current engineering muscle tissues are mainly based on immortal cell lines such as C2C12, these cell lines are typically modified to proliferate indefinitely, making them convenient for biological experiments. However, they cannot fully respond in the same way as primary cells. Nevertheless, it is difficult to obtain primary cells from aged donors or patients, and their limited proliferative capability has greatly hindered the widespread application. A robust human cell source with myogenic potential and can support long-term culture should be sorted out. The rapid development of iPSCs has offered a promising option. iPSCs possess indefinite propagation potential and can be derived from the patient directly, therefore, with preserved pathologic phenotypes. This makes the iPSCs highly attractive to pathological studies, drug screening, and as well as regenerative therapy. The integration of iPSCs and engineering technology offers great potential to generate *in vitro* models for disease modeling and therapeutic applications.

4.3. Smart biomaterials

In addition, constructs that only offer structural support are insufficient to restore functionality. Materials that provide instructive cues that could elicit desired cellular response should be formulated. Over the past decades, researchers have sought to maximize the potential therapeutic utility of cells and signaling factors by developing biomaterial-based strategies that support and guide skeletal muscle repair processes. dECM, collagen, and fibrin are leading the trends in skeletal muscle engineering. These natural materials have exhibited superior biocompatibility, while the deficiency in lot-to-lot inconsistency and the weak mechanical property of natural polymers has intrigued the scientists to develop multi-functional synthetic biomaterials with controllable properties [142,159,161,176], especially smart materials. Smart materials that are responsive to external stimuli (*e.g.*, temperature, pH, light, electric and magnetic fields) could be programmed to display desired physical and chemical properties, such as shape-changing, self-folding hydrogels or controlled degradation [240,241]. Hydrogels undergo the morphological transformation from 2D to 3D under external stimuli could be a promising strategy for mimicking skeletal muscle tissues. Given the pivotal role of bioactive molecules, for instance, growth factors, in myogenesis, smart materials could serve as a promising platform to provide stimuli-responsive delivery through designated pathways in a prescribed manner.

4.4. Proper vascularization and innervation

Vascular networks are indispensable to avoid necrosis and support long-term culture. Meanwhile, as reported by many studies, the lack of proper innervation has impeded the complete functional recovery. To integrate vascular networks and neural input would better facilitate the development and maturation of the tissue engineered skeletal muscle. The advent of 3D bioprinting technology allows the generation of simplified vascular networks out of soft hydrogels and it is of critical importance to integrate these systems together. However, given the technical limitation that the resolution of 3D bioprinting is roughly within a few hundred microns. The technical issues associated with 3D bioprinting resolution should be further investigated. Further, with the advancement of other fields, for instance, microfluidics [224,242], electrohydrodynamic printing, and so forth [243], the potential of bioprinting technology has been enlarged [244]. Filaments with higher resolution or constructs with topological cues are achievable. Taking advantage of the organoid, a SWIFT method has been proposed to generate vascular networks through direct sacrificial ink writing in the organ building blocks [245]. Inspirations could be drawn from other fabrication technologies. We envision that a synergistic system could offer a pathway to achieve tissues bearing high fidelity.

4.5. Signaling molecules/drug delivery

Besides cells and materials, a cascade of orchestrated signaling molecules are working collaboratively, such as HGF, IGF and VEGF. In addition to the growth factors, there are some small molecules have been recognized for their therapeutic potential in skeletal muscle regeneration, such as exosomes. These molecules could be encapsulated into the 3D scaffold and then delivered to the injury site. Thus, supportive biomaterials with a controllable and robust delivery manner should be developed to better release the molecules/drugs to the injury site.

5. Summary

Given the capability of capturing the complex cell-cell and cell-ECM interactions, 3D *In vitro* models hold great potential to bridge the gap between 2D monolayer culture and *in vivo* studies. Considerable progress has been achieved through a number of bioengineering technologies, as reviewed in this paper. Geometrical confinement, nanofibers, porous hydrogels, cell/growth factor delivery and bioprinting have provided profound insight into the mechanism of how cells behave in a 3D environment. Nevertheless, an engineered construct that could support multiple cells types with compliant mechanical property, necessary molecules and capable of restoring muscle function with interspersed vascular networks and adequate innervation has yet to be achieved. Particularly, further development of materials, more robust cell technology and a deeper understanding of molecular gradients in native tissue are in desperate need. We envision that with the advances in biological science, material science and burgeoning engineering technologies, better and more realistic *in vitro* models could be developed.

Declaration of competing interest

The authors declare that they have no known competing financial interests or personal relationships that could have appeared to influence the work reported in this paper.

Acknowledgements

This research is supported by the National Research Foundation, Prime Minister's Office, Singapore under its Medium-Sized Centre funding scheme.

References

[1] Karina H. Nakayama, Mahdis Shayan, Ngan F. Huang, Engineering biomimetic materials for skeletal muscle repair and regeneration, Advanced Healthcare Materials 8 (5) (2019) 1801168.
[2] Brittany L. Rodriguez, Lisa M. Larkin, Functional three-dimensional scaffolds for skeletal muscle tissue engineering, Functional 3D Tissue Engineering Scaffolds, Elsevier 2018, pp. 279–304.
[3] Benjamin T. Corona, Jessica C. Rivera, Johnny G. Owens, Joseph C. Wenke, Christopher R. Rathbone, Volumetric muscle loss leads to permanent disability following extremity trauma, Journal of Rehabilitation Research & Development 52 (7) (2015).
[4] Juan Liu, Dominik Saul, Kai Oliver Böker, Jennifer Ernst, Wolfgang Lehman, Arndt F. Schilling, Current methods for skeletal muscle tissue repair and regeneration, Biomed. Res. Int. 2018 (2018).
[5] R.G. Miller, Khema R. Sharma, Gket Pavlath, E. Gussoni, P. Yu M Mynhier, A.M. Lanctot, C.M. Greco, L. Steinman, H.M. Blau, Myoblast implantation in duchenne muscular dystrophy: the San Francisco study, Muscle & Nerve: Official Journal of the American Association of Electrodiagnostic Medicine 20 (4) (1997) 469–478.
[6] Massimiliano Cerletti, Sara Jurga, Carol A. Witczak, Michael F. Hirshman, Jennifer L. Shadrach, Laurie J. Goodyear, Amy J. Wagers, Highly efficient, functional engraftment of skeletal muscle stem cells in dystrophic muscles, Cell 134 (1) (2008) 37–47.
[7] Cheng Zhang, H.Y. Feng, S.L. Huang, J.P. Fang, L.L. Xiao, X.L. Yao, Chun Chen, X. Ye, X.L. Lu Yin Zeng, et al., Therapy of duchenne muscular dystrophy with umbilical cord blood stem cell transplantation, Zhonghua Yi Xue Yi Chuan Xue Za Zhi= Zhonghua Yixue Yichuanxue Zazhi= Chinese Journal of Medical Genetics 22 (4) (2005) 399–405.
[8] Didier Montarras, Jennifer Morgan, Charlotte Collins, Frédéric Relaix, Stéphane Zaffran, Ana Cumano, Terence Partridge, Margaret Buckingham, Direct isolation of satellite cells for skeletal muscle regeneration, Science 309 (5743) (2005) 2064–2067.

[9] Marco Quarta, Melinda Cromie, Robert Chacon, Justin Blonigan, Victor Garcia, Igor Akimenko, Mark Hamer, Patrick Paine, Merel Stok, Joseph B. Shrager, et al., Bioengineered constructs combined with exercise enhance stem cell-mediated treatment of volumetric muscle loss, Nat. Commun. 8 (2017), 15613. .

[10] Amit Aurora, Janet L. Roe, Benjamin T. Corona, Thomas J. Walters, An acellular biologic scaffold does not regenerate appreciable de novo muscle tissue in rat models of volumetric muscle loss injury, Biomaterials 67 (2015) 393–407.

[11] Jian Zhang, Zhi Qian Hu, Neill J. Turner, Shi Feng Teng, Wen Yue Cheng, Hai Yang Zhou, Li Zhang, Hong Wei Hu, Qiang Wang, Stephen F. Badylak, Perfusion-decellularized skeletal muscle as a three-dimensional scaffold with a vascular network template, Biomaterials 89 (2016) 114–126.

[12] Taimoor H. Qazi, David J. Mooney, Matthias Pumberger, Sven Geissler, Georg N. Duda, Biomaterials based strategies for skeletal muscle tissue engineering: existing technologies and future trends, Biomaterials 53 (2015) 502–521.

[13] B.H. Lee, A. Tijore, C.R.I. Lam, H. Chen, K.M. Kumar, L.P. Tan, Engineering stem cell niche and stem cell–material interactions, Smart Materials for Tissue Engineering 2016, pp. 163–196.

[14] Sólveig Thorsteinsdóttir, Marianne Deries, Ana Sofia Cachaço, Fernanda Bajanca, The extracellular matrix dimension of skeletal muscle development, Dev. Biol. 354 (2) (2011) 191–207.

[15] J.A. Trotter, P.P. Purslow, Functional morphology of the endomysium in series fibered muscles, J. Morphol. 212 (2) (1992) 109–122.

[16] Peter P. Purslow, John A. Trotter, The morphology and mechanical properties of endomysium in series-fibred muscles: variations with muscle length, Journal of Muscle Research & Cell Motility 15 (3) (1994) 299–308.

[17] Allison R. Gillies, Richard L. Lieber, Structure and function of the skeletal muscle extracellular matrix, Muscle Nerve 44 (3) (2011) 318–331.

[18] Takanori Nishimura, Role of extracellular matrix in development of skeletal muscle and postmortem aging of meat, Meat Sci. 109 (2015) 48–55.

[19] Adam J. Engler, Shamik Sen, H. Lee Sweeney, Dennis E. Discher, Matrix elasticity directs stem cell lineage specification, Cell 126 (4) (2006) 677–689.

[20] Chenyuan Gao, Lin Tang, Jieyu Hong, Chunyong Liang, Lay Poh Tan, Huaqiong Li, Effect of laser induced topography with moderate stiffness on human mesenchymal stem cell behavior, Journal of Physics: Materials 2 (3) (2019) 034006.

[21] Y. Shona Pek, Andrew C.A. Wan, Jackie Y. Ying, The effect of matrix stiffness on mesenchymal stem cell differentiation in a 3d thixotropic gel, Biomaterials 31 (3) (2010) 385–391.

[22] Andrew S. Rowlands, Peter A. George, Justin J. Cooper-White, Directing osteogenic and myogenic differentiation of mscs: interplay of stiffness and adhesive ligand presentation, Am. J. Phys. Cell Phys. 295 (4) (2008) C1037–C1044.

[23] Karl J.A. McCullagh, Rita C.R. Perlingeiro, Coaxing stem cells for skeletal muscle repair, Adv. Drug Deliv. Rev. 84 (2015) 198–207.

[24] Penney M. Gilbert, Karen L. Havenstrite, Klas E.G. Magnusson, Alessandra Sacco, Nora A. Leonardi, Peggy Kraft, Nghi K. Nguyen, Sebastian Thrun, Matthias P. Lutolf, Helen M. Blau, Substrate elasticity regulates skeletal muscle stem cell self-renewal in culture, Science 329 (5995) (2010) 1078–1081.

[25] Vahid Hosseini, Samad Ahadian, Serge Ostrovidov, Gulden Camci-Unal, Song Chen, Hirokazu Kaji, Murugan Ramalingam, Ali Khademhosseini, Engineered contractile skeletal muscle tissue on a microgrooved methacrylated gelatin substrate, Tissue Eng. A 18 (23–24) (2012) 2453–2465.

[26] Nunnapas Jiwlawat, Eileen M. Lynch, Brett N. Napiwocki, Alana Stempien, Randolph S. Ashton, Timothy J. Kamp, Wendy C. Crone, Masatoshi Suzuki, Micropatterned substrates with physiological stiffness promote cell maturation and pompe disease phenotype in human induced pluripotent stem cell-derived skeletal myocytes, Biotechnol. Bioeng. 116 (9) (2019) 2377–2392.

[27] Elena Serena, Susi Zatti, Alice Zoso, Francesca Lo Verso, F. Saverio Tedesco, Giulio Cossu, Nicola Elvassore, Skeletal muscle differentiation on a chip shows human donor mesoangioblasts' efficiency in restoring dystrophin in a duchenne muscular dystrophy model, Stem Cells Transl. Med. 5 (12) (2016) 1676–1683.

[28] Charlotte A. Collins, Irwin Olsen, Peter S. Zammit, Louise Heslop, Aviva Petrie, Terence A. Partridge, Jennifer E. Morgan, Stem cell function, self-renewal, and behavioral heterogeneity of cells from the adult muscle satellite cell niche, Cell 122 (2) (2005) 289–301.

[29] Robert W. Arpke, Radbod Darabi, Tara L. Mader, Yu Zhang, Akira Toyama, Cara-lin Lonetree, Nardina Nash, Dawn A. Lowe, Rita C.R. Perlingeiro, Michael Kyba, A new immuno-, dystrophin-deficient model, the nsg-mdx4cv mouse, provides evidence for functional improvement following allogeneic satellite cell transplantation, Stem Cells 31 (8) (2013) 1611–1620.

[30] Yusuke Ono, Luisa Boldrin, Paul Knopp, Jennifer E. Morgan, Peter S. Zammit, Muscle satellite cells are a functionally heterogeneous population in both somite-derived and branchiomeric muscles, Dev. Biol. 337 (1) (2010) 29–41.

[31] Hang Yin, Feodor Price, Michael A. Rudnicki, Satellite cells and the muscle stem cell niche, Physiol. Rev. 93 (1) (2013) 23–67.

[32] John K. Hall, Glen B. Banks, Jeffrey S. Chamberlain, Bradley B. Olwin, Prevention of muscle aging by myofiber-associated satellite cell transplantation, Sci. Transl. Med. 2 (57) (2010) 57ra83–57ra83.

[33] Jennifer L. Shadrach, Amy J. Wagers, Stem cells for skeletal muscle repair, Philosophical Transactions of the Royal Society B: Biological Sciences 366 (1575) (2011) 2297–2306.

[34] Dacha Gholobova, Melanie Gérard, Lieselot Decroix, Linda Desender, Nico Callewaert, Pieter Annaert, Lieven Thorrez, Human tissue-engineered skeletal muscle: a novel 3d in vitro model for drug disposition and toxicity after intramuscular injection, Sci. Rep. 8 (1) (2018) 12206.

[35] Teuta Domi, Emanuela Porrello, Daniele Velardo, Alessia Capotondo, Alessandra Biffi, Rossana Tonlorenzi, Stefano Amadio, Alessandro Ambrosi, Yuko Miyagoe-Suzuki, Shin 'ichi Takeda, et al., Mesoangioblast delivery of miniagrin ameliorates murine model of merosin-deficient congenital muscular dystrophy type 1a, Skelet. Muscle 5 (1) (2015) 30.

[36] Alexander Birbrair, Osvaldo Delbono, Pericytes are essential for skeletal muscle formation, Stem Cell Rev. Rep. 11 (4) (2015) 547–548.

[37] Claudia Fuoco, Elena Sangalli, Rosa Vono, Stefano Testa, Benedetto Sacchetti, Michael V.G. Latronico, Sergio Bernardini, Paolo Madeddu, Gianni Cesareni, Dror Seliktar, et al., 3d hydrogel environment rejuvenates aged pericytes for skeletal muscle tissue engineering, Front. Physiol. 5 (2014) 203.

[38] Jun Ke Zheng, Yi Wang, Aditi Karandikar, Qian Wang, Hui Gai, Ai Lian Liu, Chao Peng, Hui Zhen Sheng, Skeletal myogenesis by human embryonic stem cells, Cell Res. 16 (8) (2006) 713.

[39] Lingjun Rao, Ying Qian, Alastair Khodabukus, Thomas Ribar, Nenad Bursac, Engineering human pluripotent stem cells into a functional skeletal muscle tissue, Nat. Commun. 9 (1) (2018) 126.

[40] Sahar Ansari, Chider Chen, Xingtian Xu, Nasim Annabi, Homayoun H. Zadeh, Benjamin M. Wu, Ali Khademhosseini, Songtao Shi, Alireza Moshaverinia, Muscle tissue engineering using gingival mesenchymal stem cells encapsulated in alginate hydrogels containing multiple growth factors, Ann. Biomed. Eng. 44 (6) (2016) 1908–1920.

[41] Justus P. Beier, Franz F. Bitto, Claudia Lange, Dorothee Klumpp, Andreas Arkudas, Oliver Bleiziffer, Anja M. Boos, Raymund E. Horch, Ulrich Kneser, Myogenic differentiation of mesenchymal stem cells co-cultured with primary myoblasts, Cell Biol. Int. 35 (4) (2011) 397–406.

[42] Nadine Matthias, Samuel D. Hunt, Jianbo Wu, Jonathan Lo, Laura A. Smith Callahan, Yong Li, Johnny Huard, Radbod Darabi, Volumetric muscle loss injury repair using in situ fibrin gel cast seeded with muscle-derived stem cells (mdscs), Stem Cell Res. 27 (2018) 65–73.

[43] Min Hwan Kim, Hea Nam Hong, Joon Pio Hong, Chan Jeoung Park, Seog Woon Kwon, Soon Hee Kim, Gilson Kang, MiJung Kim, The effect of vegf on the myogenic differentiation of adipose tissue derived stem cells within thermosensitive hydrogel matrices, Biomaterials 31 (6) (2010) 1213–1218.

[44] Jonathan Mark Fishman, Athanasios Tyraskis, Panagiotis Maghsoudlou, Luca Urbani, Giorgia Totonelli, Martin A. Birchall, Paolo De Coppi, Skeletal muscle tissue engineering: which cell to use? Tissue Eng. B Rev. 19 (6) (2013) 503–515.

[45] Soumen Jana, Sheeny K. Lan Levengood, Miqin Zhang, Anisotropic materials for skeletal-muscle-tissue engineering, Adv. Mater. 28 (48) (2016) 10588–10612.

[46] S.T. Cooper, A.L. Maxwell, E. Kizana, M. Ghoddusi, E.C. Hardeman, I.E. Alexander, D.G. Allen, K.N. North, C2c12 co-culture on a fibroblast substratum enables sustained survival of contractile, highly differentiated myotubes with peripheral nuclei and adult fast myosin expression, Cell Motil. Cytoskeleton 58 (3) (2004) 200–211.

[47] Leonardo Ricotti, Toshinori Fujie, Helena Vazão, Gianni Ciofani, Roberto Marotta, Rosaria Brescia, Carlo Filippeschi, Irene Corradini, Michela Matteoli, Virgilio Mattoli, et al., Boron nitride nanotube-mediated stimulation of cell co-culture on micro-engineered hydrogels, PLoS One 8 (8) (2013), e71707. .

[48] B. Kalman, C. Monge, A. Bigot, V. Mouly, C. Picart, T. Boudou, Engineering human 3d micromuscles with co-culture of fibroblasts and myoblasts, Computer Methods in Biomechanics and Biomedical Engineering 18 (sup1) (2015) 1960–1961.

[49] Nikhil Rao, Gillie Agmon, Matthew T. Tierney, Jessica L. Ungerleider, Rebecca L. Braden, Alessandra Sacco, Karen L. Christman, Engineering an injectable muscle-specific microenvironment for improved cell delivery using a nanofibrous extracellular matrix hydrogel, ACS Nano 11 (4) (2017) 3851–3859.

[50] Michael R. Hicks, Thanh V. Cao, Paul R. Standley, Biomechanical strain vehicles for fibroblast-directed skeletal myoblast differentiation and myotube functionality in a novel coculture, Am. J. Phys. Cell Phys. 307 (8) (2014) C671–C683.

[51] Jordana Gilbert-Honick, Shama R. Iyer, Sarah M. Somers, Richard M. Lovering, Kathryn Wagner, Hai-Quan Mao, Warren L. Grayson, Engineering functional and histological regeneration of vascularized skeletal muscle, Biomaterials 164 (2018) 70–79.

[52] Karina H. Nakayama, Marco Quarta, Patrick Paine, Cynthia Alcazar, Ioannis Karakikes, Victor Garcia, Oscar J. Abilez, Nicholas S. Calvo, Chelsey S. Simmons, Thomas A. Rando, et al., Treatment of volumetric muscle loss in mice using nanofibrillar scaffolds enhances vascular organization and integration, Communications Biology 2 (1) (2019) 170.

[53] Shulamit Levenberg, Jeroen Rouwkema, Mara Macdonald, Evan S. Garfein, Daniel S. Kohane, Diane C. Darland, Robert Marini, Clemens A. Van Blitterswijk, Richard C. Mulligan, Patricia A. D'Amore, et al., Engineering vascularized skeletal muscle tissue, Nat. Biotechnol. 23 (7) (2005) 879.

[54] Shangwu Chen, Naoki Kawazoe, Guoping Chen, Biomimetic assembly of vascular endothelial cells and muscle cells in microgrooved collagen porous scaffolds, Tissue Engineering Part C: Methods 23 (6) (2017) 367–376.

[55] Yulia Shandalov, Dana Egozi, Jacob Koffler, Dekel Dado-Rosenfeld, David Ben-Shimol, Alina Freiman, Erez Shor, Aviva Kabala, Shulamit Levenberg, An engineered muscle flap for reconstruction of large soft tissue defects, Proc. Natl. Acad. Sci. 111 (16) (2014) 6010–6015.

[56] Jacob Koffler, Keren Kaufman-Francis, Yulia Shandalov, Dana Egozi, Daria Amiad Pavlov, Amir Landesberg, Shulamit Levenberg, Improved vascular organization enhances functional integration of engineered skeletal muscle grafts, Proc. Natl. Acad. Sci. 108 (36) (2011) 14789–14794.

[57] Neil R.W. Martin, Samantha L. Passey, Darren J. Player, Vivek Mudera, Keith Baar, Linda Greensmith, Mark P. Lewis, Neuromuscular junction formation in tissue-engineered skeletal muscle augments contractile function and improves cytoskeletal organization, Tissue Eng. A 21 (19–20) (2015) 2595–2604.

[58] Lisa M. Larkin, Jack H. Van Der Meulen, Robert G. Dennis, Jeffrey B. Kennedy, Functional evaluation of nerve-skeletal muscle constructs engineered in vitro, In Vitro Cellular & Developmental Biology-Animal 42 (3–4) (2006) 75–82.

[59] Yuya Morimoto, Midori Kato-Negishi, Hiroaki Onoe, Shoji Takeuchi, Three-dimensional neuron–muscle constructs with neuromuscular junctions, Biomaterials 34 (37) (2013) 9413–9419.

[60] Alec S.T. Smith, Samantha L. Passey, Neil R.W. Martin, Darren J. Player, Vivek Mudera, Linda Greensmith, Mark P. Lewis, Creating interactions between tissue-engineered skeletal muscle and the peripheral nervous system, Cells Tissues Organs 202 (3–4) (2016) 143–158.

[61] Chor Yong Tay, Scott Alexander Irvine, Freddy Y.C. Boey, Lay Poh Tan, Subbu Venkatraman, Micro−/nano-engineered cellular responses for soft tissue engineering and biomedical applications, Small 7 (10) (2011) 1361–1378.

[62] James P.K. Armstrong, Jennifer L. Puetzer, Andrea Serio, Anne Géraldine Guex, Michaella Kapnisi, Alexandre Breant, Yifan Zong, Valentine Assal, Stacey C. Skaalure, Oisn King, et al., Engineering anisotropic muscle tissue using acoustic cell patterning, Adv. Mater. 30 (43) (2018), 1802649. .

[63] Mehdi Nikkhah, Faramarz Edalat, Sam Manoucheri, Ali Khademhosseini, Engineering microscale topographies to control the cell–substrate interface, Biomaterials 33 (21) (2012) 5230–5246.

[64] Jacinthe Gingras, Robert M. Rioux, Damien Cuvelier, Nicholas A. Geisse, Jeff W. Lichtman, George M. Whitesides, L. Mahadevan, Joshua R. Sanes, Controlling the orientation and synaptic differentiation of myotubes with micropatterned substrates, Biophys. J. 97 (10) (2009) 2771–2779.

[65] Lina Altomare, Mathis Riehle, Nikolaj Gadegaard, Mariacristina Tanzi, Silvia Farè, Microcontact printing of fibronectin on a biodegradable polymeric surface for skeletal muscle cell orientation, The International journal of artificial organs 33 (8) (2010) 535–543.

[66] Yongsung Hwang, Timothy Seo, Sara Hariri, Chulmin Choi, Shyni Varghese, Matrix topographical cue-mediated myogenic differentiation of human embryonic stem cell derivatives, Polymers 9 (11) (2017) 580.

[67] Shida Miao, Margaret Nowicki, Haitao Cui, Se-Jun Lee, Xuan Zhou, David K. Mills, Lijie Grace Zhang, 4d anisotropic skeletal muscle tissue constructs fabricated by staircase effect strategy, Biofabrication 11 (3) (2019) 035030.

[68] Joseph L. Charest, Andrés J. García, William P. King, Myoblast alignment and differentiation on cell culture substrates with microscale topography and model chemistries, Biomaterials 28 (13) (2007) 2202–2210.

[69] Mainak Das, Kerry Wilson, Peter Molnar, James J. Hickman, Differentiation of skeletal muscle and integration of myotubes with silicon microstructures using serum-free medium and a synthetic silane substrate, Nat. Protoc. 2 (7) (2007) 1795.

[70] Michael S. Grigola, Casey L. Dyck, Derin S. Babacan, Danielle N. Joaquin, K. Jimmy Hsia, Myoblast alignment on 2d wavy patterns: dependence on feature characteristics and cell-cell interaction, Biotechnol. Bioeng. 111 (8) (2014) 1617–1626.

[71] Kazunori Shimizu, Hideaki Fujita, Eiji Nagamori, Alignment of skeletal muscle myoblasts and myotubes using linear micropatterned surfaces ground with abrasives, Biotechnol. Bioeng. 103 (3) (2009) 631–638.

[72] Mai T. Lam, Sylvie Sim, Xiaoyue Zhu, Shuichi Takayama, The effect of continuous wavy micropatterns on silicone substrates on the alignment of skeletal muscle myoblasts and myotubes, Biomaterials 27 (24) (2006) 4340–4347.

[73] Peng-Yuan Wang, Yu Hung-Te, Wei-Bor Tsai, Modulation of alignment and differentiation of skeletal myoblasts by submicron ridges/grooves surface structure, Biotechnol. Bioeng. 106 (2) (2010) 285–294.

[74] P. Clark, G.A. Dunn, A. Knibbs, M. Peckham, Alignment of myoblasts on ultrafine gratings inhibits fusion in vitro, Int. J. Biochem. Cell Biol. 34 (7) (2002) 816–825.

[75] Xingyu Jiang, Shuichi Takayama, Xiangping Qian, Emanuele Ostuni, Wu Hongkai, Ned Bowden, Philip LeDuc, Donald E. Ingber, George M. Whitesides, Controlling mammalian cell spreading and cytoskeletal arrangement with conveniently fabricated continuous wavy features on poly (dimethylsiloxane), Langmuir 18 (8) (2002) 3273–3280.

[76] Junggeon Park, Jang Hee Choi, Semin Kim, Inseok Jang, Sungho Jeong, Jae Young Lee, Micropatterned conductive hydrogels as multifunctional muscle-mimicking biomaterials: graphene-incorporated hydrogels directly patterned with femtosecond laser ablation, Acta Biomater. 97 (2019) 141–153.

[77] Rebecca M. Duffy, Yan Sun, Adam W. Feinberg, Understanding the role of ecm protein composition and geometric micropatterning for engineering human skeletal muscle, Ann. Biomed. Eng. 44 (6) (2016) 2076–2089.

[78] Akshata R. Naik, Sebastian Pernal, Kenneth T. Lewis, Yaobin Wu, Hongkai Wu, Nicholas J. Carruthers, Paul M. Stemmer, Bhanu P. Jena, Human skeletal muscle cells on engineered 3d platform express key growth and developmental proteins, ACS Biomaterials Science & Engineering 5 (2) (2019) 970–976.

[79] Huaqiong Li, Feng Wen, Huizhi Chen, Mintu Pal, Yuekun Lai, Allan Zijian Zhao, Lay Poh Tan, Micropatterning extracellular matrix proteins on electrospun fibrous substrate promote human mesenchymal stem cell differentiation toward neurogenic lineage, ACS Appl. Mater. Interfaces 8 (1) (2015) 563–573.

[80] Sarah M. Somers, Alexander A. Spector, Douglas J. DiGirolamo, Warren L. Grayson, Biophysical stimulation for engineering functional skeletal muscle, Tissue Eng. B Rev. 23 (4) (2017) 362–372.

[81] Kathryn W. Aguilar-Agon, Andrew J. Capel, Neil R.W. Martin, Darren J. Player, Mark P. Lewis, Mechanical loading stimulates hypertrophy in tissue-engineered skeletal muscle: molecular and phenotypic responses, J. Cell. Physiol. 234 (12) (2019) 23547–23558.

[82] Jenna L. Dziki, Ross M. Giglio, Brian M. Sicari, Derek S. Wang, Riddhi M. Gandhi, Ricardo Londono, Christopher L. Dearth, Stephen F. Badylak, The effect of mechanical loading upon extracellular matrix bioscaffold-mediated skeletal muscle remodeling, Tissue Eng. A 24 (1–2) (2018) 34–46.

[83] Lieven Thorrez, Katherine DiSano, Janet Shansky, Herman Vandenburgh, Engineering of human skeletal muscle with an autologous deposited extracellular matrix, Front. Physiol. 9 (2018).

[84] Philipp Heher, Babette Maleiner, Johanna Prüller, Andreas Herbert Teuschl, Josef Kollmitzer, Xavier Monforte, Susanne Wolbank, Heinz Redl, Dominik Rünzler, Christiane Fuchs, A novel bioreactor for the generation of highly aligned 3d skeletal muscle-like constructs through orientation of fibrin via application of static strain, Acta Biomater. 24 (2015) 251–265.

[85] Cristian Pablo Pennisi, Christian Gammelgaard Olesen, Mark de Zee, John Rasmussen, Vladimir Zachar, Uniaxial cyclic strain drives assembly and differentiation of skeletal myocytes, Tissue Eng. A 17 (19–20) (2011) 2543–2550.

[86] Wylie W. Ahmed, Tobias Wolfram, Alexandra M. Goldyn, Kristina Bruellhoff, Borja Aragüés Rioja, Martin Möller, Joachim P. Spatz, Taher A. Saif, Jürgen Groll, Ralf Kemkemer, Myoblast morphology and organization on biochemically micropatterned hydrogel coatings under cyclic mechanical strain, Biomaterials 31 (2) (2010) 250–258.

[87] N. Nikolić, S.W. Görgens, G.H. Thoresen, V. Aas, J. Eckel, K. Eckardt, Electrical pulse stimulation of cultured skeletal muscle cells as a model for in vitro exercise–possibilities and limitations, Acta Physiol. 220 (3) (2017) 310–331.

[88] Kenneth Donnelly, Alastair Khodabukus, Andrew Philp, Louise Deldicque, Robert G. Dennis, Keith Baar, A novel bioreactor for stimulating skeletal muscle in vitro, Tissue Engineering Part C: Methods 16 (4) (2010) 711–718.

[89] Karin Naumann, Dirk Pette, Effects of chronic stimulation with different impulse patterns on the expression of myosin isoforms in rat myotube cultures, Differentiation 55 (3) (1994) 203–211.

[90] Hideaki Fujita, Taku Nedachi, Makoto Kanzaki, Accelerated de novo sarcomere assembly by electric pulse stimulation in c2c12 myotubes, Exp. Cell Res. 313 (9) (2007) 1853–1865.

[91] J. Stern-Straeter, A.D. Bach, L. Stangenberg, V.T. Foerster, R.E. Horch, G.B. Stark, J.P. Beier, Impact of electrical stimulation on three-dimensional myoblast cultures-a real-time rt-pcr study, J. Cell. Mol. Med. 9 (4) (2005) 883–892.

[92] Yen-Chih Huang, Robert G. Dennis, Lisa Larkin, Keith Baar, Rapid formation of functional muscle in vitro using fibrin gels, J. Appl. Physiol. 98 (2) (2005) 706–713.

[93] Kazushi Ikeda, Akira Ito, Masanori Sato, Yoshinori Kawabe, Masamichi Kamihira, Improved contractile force generation of tissue-engineered skeletal muscle constructs by igf-i and bcl-2 gene transfer with electrical pulse stimulation, Regenerative Therapy 3 (2016) 38–44.

[94] Annie Brevet, Elaine Pinto, John Peacock, Frank E. Stockdale, Myosin synthesis increased by electrical stimulation of skeletal muscle cell cultures, Science 193 (4258) (1976) 1152–1154.

[95] Marloes L.P. Langelaan, Kristel J.M. Boonen, Kang Yuen Rosaria-Chak, Daisy W.J. van der Schaft, Mark J. Post, Frank P.T. Baaijens, Advanced maturation by electrical stimulation: differences in response between c2c12 and primary muscle progenitor cells, J. Tissue Eng. Regen. Med. 5 (7) (2011) 529–539.

[96] Alastair Khodabukus, Lauran Madden, Neel K. Prabhu, Timothy R. Koves, Christopher P. Jackman, Deborah M. Muoio, Nenad Bursac, Electrical stimulation increases hypertrophy and metabolic flux in tissue-engineered human skeletal muscle, Biomaterials 198 (2019) 259–269.

[97] Kristel J.M. Boonen, Marloes L.P. Langelaan, Roderick B. Polak, Daisy W.J. van der Schaft, Frank P.T. Baaijens, Mark J. Post, Effects of a combined mechanical stimulation protocol: value for skeletal muscle tissue engineering, J. Biomech. 43 (8) (2010) 1514–1521.

[98] Quinlyn A. Soltow, Elizabeth H. Zeanah, Vitor A. Lira, David S. Criswell, Cessation of cyclic stretch induces atrophy of c2c12 myotubes, Biochem. Biophys. Res. Commun. 434 (2) (2013) 316–321.

[99] Hiroshi Egusa, Munemasa Kobayashi, Takuya Matsumoto, Jun-Ichi Sasaki, Shinya Uraguchi, Hirofumi Yatani, Application of cyclic strain for accelerated skeletal myogenic differentiation of mouse bone marrow-derived mesenchymal stromal cells with cell alignment, Tissue Eng. A 19 (5–6) (2012) 770–782.

[100] P. Yilgor Huri, C.A. Cook, D.L. Hutton, B.C. Goh, J.M. Gimble, D.J. DiGirolamo, Warren L. Grayson, Biophysical cues enhance myogenesis of human adipose derived stem/stromal cells, Biochem. Biophys. Res. Commun. 438 (1) (2013) 180–185.

[101] Ashok Kumar, Ryan Murphy, Prema Robinson, L.E.I. Wei, Aladin M. Boriek, Cyclic mechanical strain inhibits skeletal myogenesis through activation of focal adhesion kinase, rac-1 gtpase, and nf-κb transcription factor, FASEB J. 18 (13) (2004) 1524–1535.

[102] Sung-Ho Kook, Hyun-Jeong Lee, Wan-Tae Chung, In-Ho Hwang, Seung-Ah Lee, Beom-Soo Kim, Jeong-Chae Lee, Cyclic mechanical stretch stimulates the proliferation of c2c12 myoblasts and inhibits their differentiation via prolonged activation of p38 mapk, Molecules & Cells (Springer Science & Business Media BV) 25 (4) (2008).

[103] Courtney A. Powell, Beth L. Smiley, John Mills, Herman H. Vandenburgh, Mechanical stimulation improves tissue-engineered human skeletal muscle, Am. J. Phys. Cell Phys. 283 (5) (2002) C1557–C1565.

[104] Du Geon Moon, George Christ, Joel D. Stitzel, Anthony Atala, James J. Yoo, Cyclic mechanical preconditioning improves engineered muscle contraction, Tissue Eng. A 14 (4) (2008) 473–482.

[105] Takuya Matsumoto, Jun-Ichi Sasaki, Eben Alsberg, Hiroshi Egusa, Hirofumi Yatani, Taiji Sohmura, Three-dimensional cell and tissue patterning in a strained fibrin gel system, PLoS One 2 (11) (2007), e1211. .

[106] Mollie M. Smoak, Albert Han, Emma Watson, Alysha Kishan, K. Jane Grande-Allen, Elizabeth Cosgriff-Hernandez, Antonios G. Mikos, Fabrication and characterization of electrospun decellularized muscle-derived scaffolds, Tissue Engineering Part C: Methods 25 (5) (2019) 276–287.

[107] S.Y. Severt, S.L. Maxwell, J.S. Bontrager, J.M. Leger, A.R. Murphy, Mimicking muscle fiber structure and function through electromechanical actuation of electrospun silk fiber bundles, J. Mater. Chem. B 5 (40) (2017) 8105–8114.

[108] Kristin D. McKeon-Fischer, Daniel P. Browe, Ronke M. Olabisi, Joseph W. Freeman, Poly (3, 4-ethylenedioxythiophene) nanoparticle and poly (ε-caprolactone)

electrospun scaffold characterization for skeletal muscle regeneration, J. Biomed. Mater. Res. A 103 (11) (2015) 3633–3641.
[109] Ngan F. Huang, Shyam Patel, Rahul G. Thakar, Jun Wu, Benjamin S. Hsiao, Benjamin Chu, Randall J. Lee, Song Li, Myotube assembly on nanofibrous and micropatterned polymers, Nano Lett. 6 (3) (2006) 537–542.
[110] Krishna C.R. Kolan, Jie Li, Sonya Roberts, Julie A. Semon, Jonghyun Park, Delbert E. Day, Ming-Chuan Leu, Near-field electrospinning of a polymer/bioactive glass composite to fabricate 3D biomimetic structures, Int. J. Bioprint. 5 (1) (2019).
[111] Thomas Lee Jenkins, Dianne Little, Synthetic scaffolds for musculoskeletal tissue engineering: cellular responses to fiber parameters, NPJ Regenerative medicine 4 (1) (2019) 15.
[112] A. Cai, R.E. Horch, J.P. Beier, Nanofiber composites in skeletal muscle tissue engineering, Nanofiber Composites for Biomedical Applications, Elsevier 2017, pp. 369–394.
[113] Jianxun Ding, Jin Zhang, Jiannan Li, Li Di, Chunsheng Xiao, Haihua Xiao, Huanghao Yang, Xiuli Zhuang, Xuesi Chen, Electrospun polymer biomaterials, Prog. Polym. Sci. 90 (2019) 1–34.
[114] Yanming Wang, Haigang Shi, Jing Qiao, Ye Tian, Man Wu, Wei Zhang, Yuan Lin, Zhongwei Niu, Yong Huang, Electrospun tubular scaffold with circumferentially aligned nanofibers for regulating smooth muscle cell growth, ACS Appl. Mater. Interfaces 6 (4) (2014) 2958–2962.
[115] Alexander Huber, Andy Pickett, Kevin M. Shakesheff, Reconstruction of spatially orientated myotubes in vitro using electrospun, parallel microfibre arrays, Eur Cell Mater 14 (2007) 56–63.
[116] Soumen Jana, Ashleigh Cooper, Fumio Ohuchi, Miqin Zhang, Uniaxially aligned nanofibrous cylinders by electrospinning, ACS Appl. Mater. Interfaces 4 (9) (2012) 4817–4824.
[117] Huizhi Chen, Yuan Siang Lui, Zhen Wei Tan, Justin Yin Hao Lee, Nguan Soon Tan, Lay Poh Tan, Migration and phenotype control of human dermal fibroblasts by electrospun fibrous substrates, Advanced healthcare materials 8 (9) (2019), 1801378. .
[118] Jordana Gilbert-Honick, Brian Ginn, Yuanfan Zhang, Sara Salehi, Kathryn R. Wagner, Hai-Quan Mao, Warren L. Grayson, Adipose-derived stem/stromal cells on electrospun fibrin microfiber bundles enable moderate muscle reconstruction in a volumetric muscle loss model, Cell Transplant. 27 (11) (2018) 1644–1656.
[119] Phammela N. Abarzúa-Illanes, Cristina Padilla, Andrea Ramos, Mauricio Isaacs, Jorge Ramos-Grez, Hugo C. Olgun, Loreto M. Valenzuela, Improving myoblast differentiation on electrospun poly (ε-caprolactone) scaffolds, J. Biomed. Mater. Res. A 105 (8) (2017) 2241–2251.
[120] A.G. Guex, F.M. Kocher, G. Fortunato, E. Körner, D. Hegemann, T.P. Carrel, H.T. Tevaearai, Marie-Noelle Giraud, Fine-tuning of substrate architecture and surface chemistry promotes muscle tissue development, Acta Biomater. 8 (4) (2012) 1481–1489.
[121] Megane Beldjilali-Labro, Alejandro Garcia Garcia, Firas Farhat, Fahmi Bedoui, Jean-François Grosset, Murielle Dufresne, Cécile Legallais, Biomaterials in tendon and skeletal muscle tissue engineering: current trends and challenges, Materials 11 (7) (2018) 1116.
[122] Naoya Takeda, Kenichi Tamura, Ryo Mineguchi, Yumiko Ishikawa, Yuji Haraguchi, Tatsuya Shimizu, Yusuke Hara, In situ cross-linked electrospun fiber scaffold of collagen for fabricating cell-dense muscle tissue, Journal of Artificial Organs 19 (2) (2016) 141–148.
[123] Mahsa Kheradmandi, Ebrahim Vasheghani-Farahani, Ali Ghiaseddin, Fariba Ganji, Skeletal muscle regeneration via engineered tissue culture over electrospun nanofibrous chitosan/pva scaffold, J. Biomed. Mater. Res. A 104 (7) (2016) 1720–1727.
[124] Serge Ostrovidov, Xuetao Shi, Ling Zhang, Xiaobin Liang, Sang Bok Kim, Toshinori Fujie, Murugan Ramalingam, Mingwei Chen, Ken Nakajima, Faten Al-Hazmi, et al., Myotube formation on gelatin nanofibers–multi-walled carbon nanotubes hybrid scaffolds, Biomaterials 35 (24) (2014) 6268–6277.
[125] Shuming Zhang, Liu Xi, Sebastian F. Barreto-Ortiz, Yu Yixuan, Brian P. Ginn, Nicholas A. DeSantis, Daphne L. Hutton, Warren L. Grayson, Fu-Zhai Cui, Brian A. Korgel, et al., Creating polymer hydrogel microfibres with internal alignment via electrical and mechanical stretching, Biomaterials 35 (10) (2014) 3243–3251.
[126] Yanheng Guo, Jordana Gilbert-Honick, Sarah M. Somers, Hai-Quan Mao, Warren L. Grayson, Modified cell-electrospinning for 3d myogenesis of c2c12s in aligned fibrin microfiber bundles, Biochem. Biophys. Res. Commun. 516 (2) (2019) 558–564.
[127] Shivaprasad Manchineella, Greeshma Thrivikraman, Khadija K. Khanum, Praveen C. Ramamurthy, Bikramjit Basu, T. Govindaraju, Pigmented silk nanofibrous composite for skeletal muscle tissue engineering, Advanced Healthcare Materials 5 (10) (2016) 1222–1232.
[128] Miji Yeo, GeunHyung Kim, Nano/microscale topographically designed alginate/pcl scaffolds for inducing myoblast alignment and myogenic differentiation, Carbohydr. Polym. 223 (2019), 115041. .
[129] Elizabeth M. Cronin, Frederick A. Thurmond, Rhonda Bassel-Duby, R. Sanders Williams, Woodring E. Wright, Kevin D. Nelson, Harold R. Garner, Protein-coated poly (l-lactic acid) fibers provide a substrate for differentiation of human skeletal muscle cells, Journal of Biomedical Materials Research Part A: An Official Journal of The Society for Biomaterials, The Japanese Society for Biomaterials, and The Australian Society for Biomaterials and the Korean Society for Biomaterials 69 (3) (2004) 373–381.
[130] Matthew Richard Williamson, Eric F. Adams, Allan G.A. Coombes, Gravity spun polycaprolactone fibres for soft tissue engineering: interaction with fibroblasts and myoblasts in cell culture, Biomaterials 27 (7) (2006) 1019–1026.
[131] Stefania A. Riboldi, Maurilio Sampaolesi, Peter Neuenschwander, Giulio Cossu, Sara Mantero, Electrospun degradable polyesterurethane membranes: potential scaffolds for skeletal muscle tissue engineering, Biomaterials 26 (22) (2005) 4606–4615.
[132] Jessica H. Brown, Prativa Das, Michael D. DiVito, David Ivancic, Lay Poh Tan, Jason A. Wertheim, Nanofibrous plga electrospun scaffolds modified with type i collagen influence hepatocyte function and support viability in vitro, Acta Biomater. 73 (2018) 217–227.
[133] Nor Zahari, Ruszymah Idrus, Shiplu Chowdhury, Laminin-coated poly (methyl methacrylate)(pmma) nanofiber scaffold facilitates the enrichment of skeletal muscle myoblast population, Int. J. Mol. Sci. 18 (11) (2017) 2242.
[134] Sook Hee Ku, Sahng Ha Lee, Chan Beum Park, Synergic effects of nanofiber alignment and electroactivity on myoblast differentiation, Biomaterials 33 (26) (2012) 6098–6104.
[135] Miji Yeo, Geun Hyung Kim, Anisotropically aligned cell-laden nanofibrous bundle fabricated via cell electrospinning to regenerate skeletal muscle tissue, Small 14 (48) (2018) 1803491.
[136] Qifei Jing, Jia Yan Law, Lay Poh Tan, Vadim V. Silberschmidt, Lin Li, ZhiLi Dong, Preparation, characterization and properties of polycaprolactone diol-functionalized multi-walled carbon nanotube/thermoplastic polyurethane composite, Compos. A: Appl. Sci. Manuf. 70 (2015) 8–15.
[137] Ali Abedi, Mahdi Hasanzadeh, Lobat Tayebi, Conductive nanofibrous chitosan/pedot: Pss tissue engineering scaffolds, Mater. Chem. Phys. 237 (2019), 121882. .
[138] B. Chaudhuri, B. Mondal, S. Kumar, S.C. Sarkar, Myoblast differentiation and protein expression in electrospun graphene oxide (go)-poly (ε-caprolactone, pcl) composite meshes, Mater. Lett. 182 (2016) 194–197.
[139] Simzar Hosseinzadeh, Matin Mahmoudifard, Farzaneh Mohamadyar-Toupkanlou, Masomeh Dodel, Atena Hajarizadeh, Mahdi Adabi, Masoud Soleimani, The nanofibrous pan-pani scaffold as an efficient substrate for skeletal muscle differentiation using satellite cells, Bioprocess Biosyst. Eng. 39 (7) (2016) 1163–1172.
[140] Jiazhu Xu, Ya Xie, Hongbo Zhang, Zhaoyang Ye, Wenjun Zhang, Fabrication of plga/mwnts composite electrospun fibrous scaffolds for improved myogenic differentiation of c2c12 cells, Colloids Surf. B: Biointerfaces 123 (2014) 907–915.
[141] Pathomthat Srisuk, Dillip K. Bishi, Fernanda V. Berti, Carlos J.R. Silva, Il Keun Kwon, Vitor M. Correlo, Rui L. Reis, Eumelanin nanoparticle-incorporated polyvinyl alcohol nanofibrous composite as an electroconductive scaffold for skeletal muscle tissue engineering, ACS Applied Bio Materials 1 (6) (2018) 1893–1905.
[142] Yuzhang Du, Juan Ge, Yannan Li, Peter X. Ma, Bo Lei, Biomimetic elastomeric, conductive and biodegradable polycitrate-based nanocomposites for guiding myogenic differentiation and skeletal muscle regeneration, Biomaterials 157 (2018) 40–50.
[143] Mei-Chin Chen, Yu-Chin Sun, Yuan-Hsiang Chen, Electrically conductive nanofibers with highly oriented structures and their potential application in skeletal muscle tissue engineering, Acta Biomater. 9 (3) (2013) 5562–5572.
[144] Huizhi Chen, Yan Peng, Shucheng Wu, Lay Tan, Electrospun 3d fibrous scaffolds for chronic wound repair, Materials 9 (4) (2016) 272.
[145] Jung Bok Lee, Sung In Jeong, Min Soo Bae, Dae Hyeok Yang, Dong Nyoung Heo, Chun Ho Kim, Eben Alsberg, Il Keun Kwon, Highly porous electrospun nanofibers enhanced by ultrasonication for improved cellular infiltration, Tissue Eng. A 17 (21—22) (2011) 2695–2702.
[146] Suk-Hee Park, Min Sung Kim, Byungjun Lee, Jean Ho Park, Hye Jin Lee, Nak Kyu Lee, Noo Li Jeon, Kahp-Yang Suh, Creation of a hybrid scaffold with dual configuration of aligned and random electrospun fibers, ACS Appl. Mater. Interfaces 8 (4) (2016) 2826–2832.
[147] Jin Nam, Yan Huang, Sudha Agarwal, John Lannutti, Improved cellular infiltration in electrospun fiber via engineered porosity, Tissue Eng. 13 (9) (2007) 2249–2257.
[148] Brendon M. Baker, Albert O. Gee, Robert B. Metter, Ashwin S. Nathan, Ross A. Marklein, Jason A. Burdick, Robert L. Mauck, The potential to improve cell infiltration in composite fiber-aligned electrospun scaffolds by the selective removal of sacrificial fibers, Biomaterials 29 (15) (2008) 2348–2358.
[149] Rachel Lev, Dror Seliktar, Hydrogel biomaterials and their therapeutic potential for muscle injuries and muscular dystrophies, J. R. Soc. Interface 15 (138) (2018), 20170380. .
[150] Yu Shrike Zhang, Ali Khademhosseini, Advances in engineering hydrogels, Science 356 (6337) (2017) eaaf3627.
[151] Yeong-Jin Choi, Taek Gyoung Kim, Jonghyeon Jeong, Hee-Gyeong Yi, Ji Won Park, Woonbong Hwang, Dong-Woo Cho, 3d cell printing of functional skeletal muscle constructs using skeletal muscle-derived bioink, Advanced healthcare materials 5 (20) (2016) 2636–2645.
[152] Jessica A. DeQuach, Joy E. Lin, Cynthia Cam, Hu Diane, Michael A. Salvatore, Farah Sheikh, Karen L. Christman, Injectable skeletal muscle matrix hydrogel promotes neovascularization and muscle cell infiltration in a hindlimb ischemia model, European Cells & Materials 23 (2012) 400.
[153] V. Kroehne, I. Heschel, F. Schügner, D. Lasrich, J.W. Bartsch, Harald Jockusch, Use of a novel collagen matrix with oriented pore structure for muscle cell differentiation in cell culture and in grafts, J. Cell. Mol. Med. 12 (5a) (2008) 1640–1648.
[154] Justus P. Beier, Dorothee Klumpp, Markus Rudisile, Roland Dersch, Joachim H. Wendorff, Oliver Bleiziffer, Andreas Arkudas, Elias Polykandriotis, Raymund E. Horch, Ulrich Kneser, Collagen matrices from sponge to nano: new perspectives for tissue engineering of skeletal muscle, BMC Biotechnol. 9 (1) (2009) 34.
[155] Marco Costantini, Stefano Testa, Ersilia Fornetti, Andrea Barbetta, Marcella Trombetta, Stefano Maria Cannata, Cesare Gargioli, Alberto Rainer, Engineering muscle networks in 3d gelatin methacryloyl hydrogels: influence of mechanical stiffness and geometrical confinement, Frontiers in Bioengineering and Biotechnology 5 (22) (2017).
[156] Soumen Jana, Ashleigh Cooper, Miqin Zhang, Chitosan scaffolds with unidirectional microtubular pores for large skeletal myotube generation, Advanced healthcare materials 2 (4) (2013) 557–561.

[157] Baolin Guo, Jin Qu, Xin Zhao, Mengyao Zhang, Degradable conductive self-healing hydrogels based on dextran-graft-tetraaniline and n-carboxyethyl chitosan as injectable carriers for myoblast cell therapy and muscle regeneration, Acta Biomater. 84 (2019) 180–193.
[158] Juan Martin Silva Garcia, Alyssa Panitch, Sarah Calve, Functionalization of hyaluronic acid hydrogels with ecm-derived peptides to control myoblast behavior, Acta Biomater. 84 (2019) 169–179.
[159] Emre Ergene, Betul Suyumbike Yagci, Seyda Gokyer, Abdullah Eyidogan, Eda Ayse Aksoy, Pinar Yilgor Huri, A novel polyurethane-based biodegradable elastomer as a promising material for skeletal muscle tissue engineering, Biomed. Mater. 14 (2) (2019), 025014. .
[160] Johanna Prüller, Ingra Mannhardt, Thomas Eschenhagen, Peter S. Zammit, Nicolas Figeac, Satellite cells delivered in their niche efficiently generate functional myotubes in three-dimensional cell culture, PLoS One 13 (9) (2018), e0202574. .
[161] Woojin M. Han, Shannon E. Anderson, Mahir Mohiuddin, Daniela Barros, Shadi A. Nakhai, Eunjung Shin, Isabel Freitas Amaral, Ana Paula Pêgo, Andrés J. García, Young C. Jang, Synthetic matrix enhances transplanted satellite cell engraftment in dystrophic and aged skeletal muscle with comorbid trauma, Sci. Adv. 4 (8) (2018) eaar4008.
[162] J.A. Passipieri, H.B. Baker, Mevan Siriwardane, Mary D. Ellenburg, Manasi Vadhavkar, Justin M. Saul, Seth Tomblyn, Luke Burnett, George J. Christ, Keratin hydrogel enhances in vivo skeletal muscle function in a rat model of volumetric muscle loss, Tissue Eng. A 23 (11−12) (2017) 556–571.
[163] H.B. Baker, J.A. Passipieri, Mevan Siriwardane, Mary D. Ellenburg, Manasi Vadhavkar, Christopher R. Bergman, Justin M. Saul, Seth Tomblyn, Luke Burnett, George J. Christ, Cell and growth factor-loaded keratin hydrogels for treatment of volumetric muscle loss in a mouse model, Tissue Eng. A 23 (11–12) (2017) 572–584.
[164] Aline Bauer, Luo Gu, Brian Kwee, Weiwei Aileen Li, Maxence Dellacherie, Adam D. Celiz, David J. Mooney, Hydrogel substrate stress-relaxation regulates the spreading and proliferation of mouse myoblasts, Acta Biomater. 62 (2017) 82–90.
[165] Eva Kildall Hejbøl, Jeeva Sellathurai, Prabha Damodaran Nair, Henrik Daa Schrøder, Injectable scaffold materials differ in their cell instructive effects on primary human myoblasts, Journal of tissue engineering (2017) 8 2041731417717677.
[166] Beth E. Pollot, Christopher R. Rathbone, Joseph C. Wenke, Teja Guda, Natural polymeric hydrogel evaluation for skeletal muscle tissue engineering, J. Biomed. Mater. Res. B Appl. Biomater. 106 (2) (2018) 672–679.
[167] Yeong-Jin Choi, Young-Joon Jun, Dong Yeon Kim, Hee-Gyeong Yi, Su-Hun Chae, Junsu Kang, Juyong Lee, Gao Ge, Jeong-Sik Kong, Jinah Jang, et al., A 3d cell printed muscle construct with tissue-derived bioink for the treatment of volumetric muscle loss, Biomaterials 206 (2019) 160–169.
[168] Mark Juhas, Nenad Bursac, Roles of adherent myogenic cells and dynamic culture in engineered muscle function and maintenance of satellite cells, Biomaterials 35 (35) (2014) 9438–9446.
[169] Ji Hyun Kim, In Kap Ko, Anthony Atala, James J. Yoo, Progressive muscle cell delivery as a solution for volumetric muscle defect repair, Sci. Rep. 6 (2016) 38754.
[170] Raymond L. Page, Christopher Malcuit, Lucy Vilner, Ina Vojtic, Sharon Shaw, Emmett Hedblom, Jason Hu, George D. Pins, Marsha W. Rolle, Tanja Dominko, Restoration of skeletal muscle defects with adult human cells delivered on fibrin microthreads, Tissue Eng. A 17 (21–22) (2011) 2629–2640.
[171] Stéphane Chiron, Carole Tomczak, Alain Duperray, Jeanne Lainé, Gisèle Bonne, Alexandra Eder, Arne Hansen, Thomas Eschenhagen, Claude Verdier, Catherine Coirault, Complex interactions between human myoblasts and the surrounding 3d fibrin-based matrix, PLoS One 7 (4) (2012), e36173. .
[172] Sara Hinds, Weining Bian, Robert G. Dennis, Nenad Bursac, The role of extracellular matrix composition in structure and function of bioengineered skeletal muscle, Biomaterials 32 (14) (2011) 3575–3583.
[173] Weining Bian, Nenad Bursac, Engineered skeletal muscle tissue networks with controllable architecture, Biomaterials 30 (7) (2009) 1401–1412.
[174] Dacha Gholobova, Lieselot Decroix, Vicky Van Muylder, Linda Desender, Melanie Gerard, Gilles Carpentier, Herman Vandenburgh, Lieven Thorrez, Endothelial network formation within human tissue-engineered skeletal muscle, Tissue Eng. A 21 (19–20) (2015) 2548–2558.
[175] Chieh Mei, Chih-Wei Chao, Che-Wei Lin, Shing Tak Li, Kuan-Han Wu, Kai-Chiang Yang, Jiashing Yu, Three-dimensional spherical gelatin bubble-based scaffold improves the myotube formation of h9c2 myoblasts, Biotechnol. Bioeng. 116 (5) (2019) 1190–1200.
[176] Francesca Gattazzo, Carmelo De Maria, Alessandro Rimessi, Silvia Donà, Paola Braghetta, Paolo Pinton, Giovanni Vozzi, Paolo Bonaldo, Gelatin–genipin-based biomaterials for skeletal muscle tissue engineering, J. Biomed. Mater. Res. B Appl. Biomater. 106 (8) (2018) 2763–2777.
[177] Serge Ostrovidov, Samad Ahadian, Javier Ramon-Azcon, Vahid Hosseini, Toshinori Fujie, S. Prakash Parthiban, Hitoshi Shiku, Tomokazu Matsue, Hirokazu Kaji, Murugan Ramalingam, et al., Three-dimensional co-culture of c2c12/pc12 cells improves skeletal muscle tissue formation and function, J. Tissue Eng. Regen. Med. 11 (2) (2017) 582–595.
[178] Javier Ramón-Azcón, Samad Ahadian, Mehdi Estili, Xiaobin Liang, Serge Ostrovidov, Hirokazu Kaji, Hitoshi Shiku, Murugan Ramalingam, Ken Nakajima, Yoshio Sakka, et al., Dielectrophoretically aligned carbon nanotubes to control electrical and mechanical properties of hydrogels to fabricate contractile muscle myofibers, Adv. Mater. 25 (29) (2013) 4028–4034.
[179] Samad Ahadian, Javier Ramón-Azcón, Mehdi Estili, Xiaobin Liang, Serge Ostrovidov, Hitoshi Shiku, Murugan Ramalingam, Ken Nakajima, Yoshio Sakka, Hojae Bae, et al., Hybrid hydrogels containing vertically aligned carbon nanotubes with anisotropic electrical conductivity for muscle myofiber fabrication, Sci. Rep. 4 (2014) 4271.
[180] Stephanie L. Hume, Sarah M. Hoyt, John S. Walker, Balaji V. Sridhar, John F. Ashley, Christopher N. Bowman, Stephanie J. Bryant, Alignment of multi-layered muscle cells within three-dimensional hydrogel macrochannels, Acta Biomater. 8 (6) (2012) 2193–2202.
[181] Sung Ho Cha, Hyun Jong Lee, Won-Gun Koh, Study of myoblast differentiation using multi-dimensional scaffolds consisting of nano and micropatterns, Biomaterials research 21 (1) (2017) 1.
[182] Ruonan Dong, Xin Zhao, Baolin Guo, Peter X. Ma, Biocompatible elastic conductive films significantly enhanced myogenic differentiation of myoblast for skeletal muscle regeneration, Biomacromolecules 18 (9) (2017) 2808–2819.
[183] Apoorva S. Salimath, Andrés J. García, Biofunctional hydrogels for skeletal muscle constructs, J. Tissue Eng. Regen. Med. 10 (11) (2016) 967–976.
[184] Ling Wang, Yaobin Wu, Baolin Guo, Peter X. Ma, Nanofiber yarn/hydrogel core–shell scaffolds mimicking native skeletal muscle tissue for guiding 3d myoblast alignment, elongation, and differentiation, ACS Nano 9 (9) (2015) 9167–9179.
[185] Claudia Fuoco, Maria Lavinia Salvatori, Antonella Biondo, Keren Shapira-Schweitzer, Sabrina Santoleri, Stefania Antonini, Sergio Bernardini, Francesco Saverio Tedesco, Stefano Cannata, Dror Seliktar, et al., Injectable polyethylene glycol-fibrinogen hydrogel adjuvant improves survival and differentiation of transplanted mesoangioblasts in acute and chronic skeletal-muscle degeneration, Skelet. Muscle 2 (1) (2012) 24.
[186] Carlo Alberto Rossi, Marina Flaibani, Bert Blaauw, Michela Pozzobon, Elisa Figallo, Carlo Reggiani, Libero Vitiello, Nicola Elvassore, Paolo De Coppi, In vivo tissue engineering of functional skeletal muscle by freshly isolated satellite cells embedded in a photopolymerizable hydrogel, FASEB J. 25 (7) (2011) 2296–2304.
[187] Kevin J. De France, Kevin G. Yager, Katelyn J.W. Chan, Brandon Corbett, Emily D. Cranston, Todd Hoare, Injectable anisotropic nanocomposite hydrogels direct in situ growth and alignment of myotubes, Nano Lett. 17 (10) (2017) 6487–6495.
[188] Hug Aubin, Jason W. Nichol, Ché B. Hutson, Hojae Bae, Alisha L. Sieminski, Donald M. Cropek, Payam Akhyari, Ali Khademhosseini, Directed 3d cell alignment and elongation in microengineered hydrogels, Biomaterials 31 (27) (2010) 6941–6951.
[189] A.S.T. Smith, S. Passey, L. Greensmith, V. Mudera, M.P. Lewis, Characterization and optimization of a simple, repeatable system for the long term in vitro culture of aligned myotubes in 3d, J. Cell. Biochem. 113 (3) (2012) 1044–1053.
[190] Michiel W. Pot, Kaeuis A. Faraj, Alaa Adawy, Willem J.P. van Enckevort, Herman T.B. van Moerkerk, Elias Vlieg, Willeke F. Daamen, Toin H. van Kuppevelt, Versatile wedge-based system for the construction of unidirectional collagen scaffolds by directional freezing: practical and theoretical considerations, ACS Appl. Mater. Interfaces 7 (16) (2015) 8495–8505.
[191] Mokit Chau, Kevin J. De France, Bernd Kopera, Vanessa R. Machado, Sabine Rosenfeldt, Laura Reyes, Katelyn J.W. Chan, Stephan Förster, Emily D. Cranston, Todd Hoare, et al., Composite hydrogels with tunable anisotropic morphologies and mechanical properties, Chem. Mater. 28 (10) (2016) 3406–3415.
[192] Daming Wang, Frederik Romer, Louise Connell, Claudia Walter, Eduardo Saiz, Sheng Yue, Peter D. Lee, David S. McPhail, John V. Hanna, Julian R. Jones, Highly flexible silica/chitosan hybrid scaffolds with oriented pores for tissue regeneration, J. Mater. Chem. B 3 (38) (2015) 7560–7576.
[193] Kazuya Furusawa, Shoichi Sato, Jyun-ichi Masumoto, Yohei Hanazaki, Yasuyuki Maki, Toshiaki Dobashi, Takao Yamamoto, Akimasa Fukui, Naoki Sasaki, Studies on the formation mechanism and the structure of the anisotropic collagen gel prepared by dialysis-induced anisotropic gelation, Biomacromolecules 13 (1) (2011) 29–39.
[194] Ji Hyun Kim, Young-Joon Seol, In Kap Ko, Hyun-Wook Kang, Young Koo Lee, James J. Yoo, Anthony Atala, Sang Jin Lee, 3d bioprinted human skeletal muscle constructs for muscle function restoration, Sci. Rep. 8 (2018).
[195] Xinxin Zhao, Yuan Siang Lui, Caleb Kai Chuen Choo, Wan Ting Sow, Charlotte Liwen Huang, Kee Woei Ng, Lay Poh Tan, Joachim Say Chye Loo, Calcium phosphate coated keratin–pcl scaffolds for potential bone tissue regeneration, Mater. Sci. Eng. C 49 (2015) 746–753.
[196] S. Deepthi, K. Jeevitha, M. Nivedhitha Sundaram, K.P. Chennazhi, R. Jayakumar, Chitosan–hyaluronic acid hydrogel coated poly (caprolactone) multiscale bilayer scaffold for ligament regeneration, Chem. Eng. J. 260 (2015) 478–485.
[197] Lucy A. Bosworth, Lesley-Anne Turner, Sarah H. Cartmell, State of the art composites comprising electrospun fibres coupled with hydrogels: a review, Nanomedicine 9 (3) (2013) 322–335.
[198] Soumen Jana, Matthew Leung, Julia Chang, Miqin Zhang, Effect of nano-and micro-scale topological features on alignment of muscle cells and commitment of myogenic differentiation, Biofabrication 6 (3) (2014), 035012. .
[199] Ying Yang, Ian Wimpenny, Mark Ahearne, Portable nanofiber meshes dictate cell orientation throughout three-dimensional hydrogels, Nanomedicine 7 (2) (2011) 131–136.
[200] Rishma Shah, Jonathan C. Knowles, Nigel P. Hunt, Mark P. Lewis, Development of a novel smart scaffold for human skeletal muscle regeneration, J. Tissue Eng. Regen. Med. 10 (2) (2016) 162–171.
[201] Wei Long Ng, Chee Kai Chua, Yu-Fang Shen, Print me an organ! Why we are not there yet, Prog. Polym. Sci. (2019) 101145.
[202] Wei Zhu, Haitao Cui, Benchaa Boualam, Fahed Masood, Erin Flynn, Raj D. Rao, Zhi-Yong Zhang, Lijie Grace Zhang, 3d bioprinting mesenchymal stem cell-laden construct with core–shell nanospheres for cartilage tissue engineering, Nanotechnology 29 (18) (2018), 185101. .
[203] Anni Sorkio, Lothar Koch, Laura Koivusalo, Andrea Deiwick, Susanna Miettinen, Boris Chichkov, Heli Skottman, Human stem cell based corneal tissue mimicking structures using laser-assisted 3d bioprinting and functional bioinks, Biomaterials 171 (2018) 57–71.
[204] Yuxiao Lai, Li Ye, Huijuan Cao, Jing Long, Xinluan Wang, Long Li, Cairong Li, Qingyun Jia, Bin Teng, Tingting Tang, et al., Osteogenic magnesium incorporated

into plga/tcp porous scaffold by 3d printing for repairing challenging bone defect, Biomaterials 197 (2019) 207–219.
[205] Yu Shrike Zhang, Andrea Arneri, Simone Bersini, Su-Ryon Shin, Kai Zhu, Zahra Goli-Malekabadi, Julio Aleman, Cristina Colosi, Fabio Busignani, Valeria Dell'Erba, et al., Bioprinting 3d microfibrous scaffolds for engineering endothelialized myocardium and heart-on-a-chip, Biomaterials 110 (2016) 45–59.
[206] Pei Zhuang, Alfred Xuyang Sun, Jia An, Chee Kai Chua, Sing Yian Chew, 3d neural tissue models: from spheroids to bioprinting, Biomaterials 154 (2018) 113–133.
[207] Amir K. Miri, Akbar Khalilpour, Berivan Cecen, Sushila Maharjan, Su Ryon Shin, Ali Khademhosseini, Multiscale bioprinting of vascularized models, Biomaterials 198 (2019) 204–216.
[208] Bagrat Grigoryan, Samantha J. Paulsen, Daniel C. Corbett, Daniel W. Sazer, Chelsea L. Fortin, Alexander J. Zaita, Paul T. Greenfield, Nicholas J. Calafat, John P. Gounley, Anderson H. Ta, et al., Multivascular networks and functional intravascular topologies within biocompatible hydrogels, Science 364 (6439) (2019) 458–464.
[209] Serge Ostrovidov, Sahar Salehi, Marco Costantini, Kasinan Suthiwanich, Majid Ebrahimi, Ramin Banan Sadeghian, Toshinori Fujie, Xuetao Shi, Stefano Cannata, Cesare Gargioli, et al., 3d bioprinting in skeletal muscle tissue engineering, Small 15 (24) (2019), 1805530. .
[210] Pei Zhuang, Wei Long Ng, Jia An, Chee Kai Chua, Lay Poh Tan, Layer-by-layer ultraviolet assisted extrusion-based (uae) bioprinting of hydrogel constructs with high aspect ratio for soft tissue engineering applications, PLoS One 14 (6) (2019), e0216776. .
[211] Sean V. Murphy, Anthony Atala, 3d bioprinting of tissues and organs, Nat. Biotechnol. 32 (8) (2014) 773.
[212] Wei Long Ng, Jia Min Lee, Wai Yee Yeong, May Win Naing, Microvalve-based bioprinting–process, bio-inks and applications, Biomaterials science 5 (4) (2017) 632–647.
[213] Miaomiao Zhou, Bae Hoon Lee, Yu Jun Tan, Lay Poh Tan, Microbial transglutaminase induced controlled crosslinking of gelatin methacryloyl to tailor rheological properties for 3d printing, Biofabrication 11 (2) (2019), 025011. .
[214] Miaomiao Zhou, Bae Hoon Lee, Lay Poh Tan, A dual crosslinking strategy to tailor rheological properties of gelatin methacryloyl, International Journal of Bioprinting 3 (2) (2017) 130–137.
[215] Miji Yeo, GeunHyung Kim, Three-dimensional microfibrous bundle structure fabricated using an electric field-assisted/cell printing process for muscle tissue regeneration, ACS Biomaterials Science & Engineering 4 (2) (2018) 728–738.
[216] WonJin Kim, GeunHyung Kim, A functional bioink and its application in myoblast alignment and differentiation, Chem. Eng. J. 366 (2019) 150–162.
[217] Tyler K. Merceron, Morgan Burt, Young-Joon Seol, Hyun-Wook Kang, Sang Jin Lee, James J. Yoo, Anthony Atala, A 3d bioprinted complex structure for engineering the muscle–tendon unit, Biofabrication 7 (3) (2015), 035003. .
[218] Hyun-Wook Kang, Sang Jin Lee, In Kap Ko, Carlos Kengla, James J. Yoo, Anthony Atala, A 3d bioprinting system to produce human-scale tissue constructs with structural integrity, Nat. Biotechnol. 34 (3) (2016) 312.
[219] Ji Hyun Kim, Ickhee Kim, Young-Joon Seol, In Kap Ko, James J. Yoo, Anthony Atala, Sang Jin Lee, Neural cell integration into 3d bioprinted skeletal muscle constructs accelerates restoration of muscle function, Nat. Commun. 11 (1) (2020) 1–12.
[220] Miji Yeo, Hyeongjin Lee, Geun Hyung Kim, Combining a micro/nano-hierarchical scaffold with cell-printing of myoblasts induces cell alignment and differentiation favorable to skeletal muscle tissue regeneration, Biofabrication 8 (3) (2016), 035021. .
[221] Gi Hoon Yang, JiUn Lee, GeunHyung Kim, The fabrication of uniaxially aligned micro-textured polycaprolactone struts and application for skeletal muscle tissue regeneration, Biofabrication 11 (2) (2019), 025005. .
[222] Miji Yeo, GeunHyung Kim, Micro/nano-hierarchical scaffold fabricated using a cell electrospinning/3d printing process for co-culturing myoblasts and huvecs to induce myoblast alignment and differentiation, Acta Biomater. 107 (2020) 102–114.
[223] WonJin Kim, Minseong Kim, Geun Hyung Kim, 3d-printed biomimetic scaffold simulating microfibril muscle structure, Adv. Funct. Mater. 28 (26) (2018) 1800405.
[224] Marco Costantini, Stefano Testa, Pamela Mozetic, Andrea Barbetta, Claudia Fuoco, Ersilia Fornetti, Francesco Tamiro, Sergio Bernardini, Wojciech Jaroszewicz, Jakub, et al., Microfluidic-enhanced 3d bioprinting of aligned myoblast-laden hydrogels leads to functionally organized myofibers in vitro and in vivo, Biomaterials 131 (2017) 98–110.
[225] Minseong Kim, WonJin Kim, GeunHyung Kim, Topologically micropatterned collagen and poly (ε-caprolactone) struts fabricated using the poly (vinyl alcohol) fibrillation/leaching process to develop efficiently engineered skeletal muscle tissue, ACS Appl. Mater. Interfaces 9 (50) (2017) 43459–43469.
[226] WonJin Kim, Hyeongjin Lee, JiUn Lee, Anthony Atala, James J. Yoo, Sang Jin Lee, Geun Hyung Kim, Efficient myotube formation in 3d bioprinted tissue construct by biochemical and topographical cues, Biomaterials 230 (2020), 119632. .
[227] Eric Lepowsky, Savas Tasoglu, 3d printing for drug manufacturing: a perspective on the future of pharmaceuticals, Int J Bioprint 4 (1) (2018) 119.
[228] Kuen Yong Lee, Martin C. Peters, Kenneth W. Anderson, David J. Mooney, Controlled growth factor release from synthetic extracellular matrices, Nature 408 (6815) (2000) 998.
[229] Viktoriya Y. Rybalko, Chantal B. Pham, Pei-Ling Hsieh, David W. Hammers, Melissa Merscham-Banda, Laura J. Suggs, Roger P. Farrar, Controlled delivery of sdf-1α and igf-1: Cxcr4+ cell recruitment and functional skeletal muscle recovery, Biomaterials Science 3 (11) (2015) 1475–1486.
[230] Jonathan M. Grasman, Michelle J. Zayas, Raymond L. Page, George D. Pins, Biomimetic scaffolds for regeneration of volumetric muscle loss in skeletal muscle injuries, Acta Biomater. 25 (2015) 2–15.
[231] Cristina Borselli, Hannah Storrie, Frank Benesch-Lee, Dmitry Shvartsman, Christine Cezar, Jeff W. Lichtman, Herman H. Vandenburgh, David J. Mooney, Functional muscle regeneration with combined delivery of angiogenesis and myogenesis factors, Proc. Natl. Acad. Sci. 107 (8) (2010) 3287–3292.
[232] E.A. Silva, David J. Mooney, Spatiotemporal control of vascular endothelial growth factor delivery from injectable hydrogels enhances angiogenesis, J. Thromb. Haemost. 5 (3) (2007) 590–598.
[233] Bridget M. Deasy, Joseph M. Feduska, Thomas R. Payne, Yong Li, Fabrisia Ambrosio, Johnny Huard, Effect of vegf on the regenerative capacity of muscle stem cells in dystrophic skeletal muscle, Mol. Ther. 17 (10) (2009) 1788–1798.
[234] Elliott Hill, Tanyarut Boontheekul, David J. Mooney, Regulating activation of transplanted cells controls tissue regeneration, Proc. Natl. Acad. Sci. 103 (8) (2006) 2494–2499.
[235] Cristina Borselli, Christine A. Cezar, Dymitri Shvartsman, Herman H. Vandenburgh, David J. Mooney, The role of multifunctional delivery scaffold in the ability of cultured myoblasts to promote muscle regeneration, Biomaterials 32 (34) (2011) 8905–8914.
[236] Andrea García-Lizarribar, Xiomara Fernández-Garibay, Ferran Velasco-Mallorqu, Albert G. Castaño, Josep Samitier, Javier Ramon-Azcon, Composite biomaterials as long-lasting scaffolds for 3d bioprinting of highly aligned muscle tissue, Macromol. Biosci. 18 (10) (2018), 1800167. .
[237] Xiaofeng Cui, Guifang Gao, Yongjun Qiu, Accelerated myotube formation using bioprinting technology for biosensor applications, Biotechnol. Lett. 35 (3) (2013) 315–321.
[238] Wafaa Arab, Sakandar Rauf, Ohoud Al-Harbi, Charlotte A.E. Hauser, Novel ultrashort self-assembling peptide bioinks for 3d culture of muscle myoblast cells, Int. J. Bioprint. 4 (2018) 129.
[239] Wafaa Arab, Kowther Kahin, Zainab Khan, Charlotte Hauser, Exploring nanofibrous self-assembling peptide hydrogels using mouse myoblast cells for three dimensional bioprinting and tissue engineering applications, Int. J. Bioprint. 5 (2) (2019).
[240] Lorenzo Vannozzi, Immihan Ceren Yasa, Hakan Ceylan, Arianna Menciassi, Leonardo Ricotti, Metin Sitti, Self-folded hydrogel tubes for implantable muscular tissue scaffolds, Macromol. Biosci. 18 (4) (2018), 1700377. .
[241] Kwanghyun Baek, Jae Hyun Jeong, Artem Shkumatov, Rashid Bashir, Hyunjoon Kong, In situ self-folding assembly of a multi-walled hydrogel tube for uniaxial sustained molecular release, Adv. Mater. 25 (39) (2013) 5568–5573.
[242] Cristina Colosi, Su Ryon Shin, Vijayan Manoharan, Solange Massa, Marco Costantini, Andrea Barbetta, Mehmet Remzi Dokmeci, Mariella Dentini, Ali Khademhosseini, Microfluidic bioprinting of heterogeneous 3d tissue constructs using low-viscosity bioink, Adv. Mater. 28 (4) (2016) 677–684.
[243] Hongtao Liang, Jiankang He, Jinke Chang, Bing Zhang, Dichen Li, Coaxial nozzle-assisted electrohydrodynamic printing for microscale 3d cell-laden constructs, Int. J. Bioprint. 4 (2018) 1–8.
[244] Y. Zhang, Three-dimensional-printing for microfluidics or the other way around? Int. J. Bioprint. 5 (2) (2019) 192.
[245] Mark A. Skylar-Scott, Sebastien G.M. Uzel, Lucy L. Nam, John H. Ahrens, Ryan L. Truby, Sarita Damaraju, Jennifer A. Lewis, Biomanufacturing of organ-specific tissues with high cellular density and embedded vascular channels, Sci. Adv. 5 (9) (2019), eaaw2459. .